

Bayesian Test for Colocalisation Between Pairs of Genetic Association Studies Using Summary Statistics

Claudia Giambartolomei^{1,*}, Damjan Vukcevic², Eric E. Schadt³, Lude Franke⁴, Aroon D. Hingorani⁵, Chris Wallace⁶, Vincent Plagnol¹

1 UCL Genetics Institute, University College London (UCL), Darwin Building, Gower Street, London WC1E 6BT, UK

2 Murdoch Childrens Research Institute, Royal Children's Hospital, Melbourne, Australia

3 Department of Genetics and Genomics Sciences, Mount Sinai School of Medicine, New York, New York, United States of America

4 Department of Genetics, University Medical Center Groningen, University of Groningen, Groningen, The Netherlands

5 Institute of Cardiovascular Science, University College London, London WC1E 6BT, UK

6 JDRF/Wellcome Trust Diabetes and Inflammation Laboratory, Cambridge, Institute for Medical Research, Department of Medical Genetics, NIHR, Cambridge Biomedical Research Centre, University of Cambridge, Addenbrooke's Hospital, Hills Rd, Cambridge, CB2 0XY, UK

* E-mail: claudia.giambartolomei.10@ucl.ac.uk

Abstract

Genetic association studies, in particular the genome-wide association study (GWAS) design, have provided a wealth of novel insights into the aetiology of a wide range of human diseases and traits, in particular cardiovascular diseases and lipid biomarkers. The next challenge consists of understanding the molecular basis of these associations. The integration of multiple association datasets, including gene expression datasets, can contribute to this goal. We have developed a novel statistical methodology to assess whether two association signals are consistent with a shared causal variant. An application is the integration of disease scans with expression quantitative trait locus (eQTL) studies, but any pair of GWAS datasets can be integrated in this framework. We demonstrate the value of the approach by re-analysing a gene expression dataset in 966 liver samples with a published meta-analysis of lipid traits including > 100,000 individuals of European ancestry [1]. Combining all lipid biomarkers, our re-analysis supported 29 out of 38 reported colocalisation results with eQTLs and identified 14 new colocalisation results, hence highlighting the value of a formal statistical test. In two cases of reported eQTL-lipid pairs (*IFT172*, *TBKBP1*) for which our analysis suggests that the eQTL pattern is not consistent with the lipid association, we identify alternative colocalisation results with *GCKR* and *KPNB1*, indicating that these genes are more likely to be the causal in these genomic intervals. A key feature of the method is the ability to derive the output statistics from single SNP summary statistics, hence making it possible to perform systematic meta-analysis type comparisons across multiple GWAS datasets (implemented online at <http://coloc.cs.ucl.ac.uk/coloc/>). Our methodology provides information about candidate causal genes in associated intervals and has direct implications for the understanding of complex diseases as well as the design of drugs to target disease pathways.

Author Summary

Genome-wide association studies (GWAS) have found a large number of genetic regions (“loci”) affecting clinical end-points and phenotypes, many outside coding intervals. One approach to understanding the biological basis of these associations has been to explore whether GWAS signals from intermediate cellular phenotypes, in particular gene expression, are located in the same loci (“colocalise”) and are potentially mediating the disease signals. However it is not clear how to assess whether the same variants are

responsible for the two GWAS signals or whether it is distinct causal variants close to each other. In this paper, we describe a statistical method which can use simply single variant summary statistics to test for colocalisation of GWAS signals. We describe one application of our method to a meta-analysis of blood lipids and liver expression, although any two datasets resulting from association studies can be used. Our method is able to detect the subset of GWAS signals explained by regulatory effects and identify candidate genes affected by the same GWAS variants. As summary GWAS data are increasingly available, applications of colocalisation methods to integrate the findings will be essential for functional follow-up, and will also be particularly useful to identify tissue specific signals in eQTL datasets.

Introduction

In the last decade, hundreds of genomic loci affecting complex diseases and disease relevant intermediate phenotypes have been found and robustly replicated using genome-wide association studies (GWAS, [2]). At the same time, gene expression measurements derived from microarray [3] or RNA sequencing [4] studies have been used extensively as an outcome trait for the GWAS design. Such studies are usually referred to as expression quantitative trait locus (eQTL) analysis. While GWAS datasets have provided a steady flow of positive and replicable results, the interpretation of these findings, and in particular the identification of underlying molecular mechanisms, has proven to be challenging. Integrating molecular level data and other disease relevant intermediate phenotypes with GWAS results is the natural step forward in order to understand the biological relevance of these results.

In this context, a natural question to ask is whether two independent association signals at the same locus, typically generated by two GWAS studies, are consistent with a shared causal variant. If the answer is positive, we refer to this situation as colocalised traits, and the likelihood that both traits share a causal mechanism is greatly increased. A typical example involves an eQTL study and a disease association result, which points to the causal gene and the tissue in which the effect is mediated [5–7]. The same questions can also be considered between pairs of eQTLs [8, 9], or pairs of diseases [10].

However, identifying the traits that share a common association signal is not a trivial statistical task. Visual comparison of overlaps of association signals with an expression dataset is a step in this direction (using for example Sanger tool Genevar <http://www.sanger.ac.uk/resources/software/genevar/>), but the abundance of eQTLs in the human genome and across different tissues makes an accidental overlap between these signals very likely [3]. Therefore visual comparison is not enough to make inferences about causality and formal statistical tests must be used to address this question.

Nica et al. [5] proposed a methodology to rank the SNPs with an influence on two traits based on the residual association conditional on the most associated SNP. By comparing the GWAS SNP score with all other SNPs in the associated region, this method accounts for the local LD structure. However this is not a formal test of a null hypothesis for, or against, colocalisation at the locus of interest. A formal test of colocalisation has been developed in a regression framework. This is based on testing a null hypothesis of proportionality of regression coefficients for two traits across any set of SNPs, an assumption which should hold whenever they share causal variant(s) [11, 12]. No assumption is made about the number of causal variants, although the method does assume that in the case of multiple causal variants, all are shared. However, both Nica’s ranking method and proportionality testing share the drawback of having to specify a subset of SNPs to base the test on, and Wallace [13] shows that this step can generate significant biases. The main sources of bias are overestimation of effect sizes at selected SNPs (termed “Winner’s curse”), and the fact that, owing to random fluctuations, the causal variant may not always be the most strongly associated one. These factors lead to rejection of colocalisation in situations where the causal SNP is in fact shared. Although this can be overcome in the case of proportionality testing by averaging over the uncertainty associated with the best SNP models [13], perhaps the greatest limitation is the requirement for individual level genotype data, which are rarely available for large scale eQTL datasets.

The success of GWAS meta-analyses has shown that there is considerable benefit in being able to derive association tests on the basis of summary statistics. With these advantages in mind, He et al. [7] developed a statistical test to match the pattern of gene expression with a GWAS dataset. This approach, coded in the software Sherlock, can accommodate p -values as input. However, their hypothesis of interest differs from the question of colocalisation, with the focus of the method being on genomewide convergence of signals, assuming an abundance of trans eQTLs. In particular, SNPs that are not associated with gene expression do not contribute to the test statistic. Such variants can provide strong evidence against colocalisation if they are strongly associated with the GWAS outcome.

These limitations motivate the development of novel methodologies to test for colocalisation between pairs of traits. Here, we derive a novel Bayesian statistical test for colocalisation that addresses many of the shortcomings of existing tools. Our analysis focuses on a single genomic region at a time, with a major focus on interpreting the pattern of LD at that locus.

Our underlying model is closely related to the approach developed by Flutre et al. [9], which considers the different but related problem of maximising the power to discover eQTLs in expression datasets of multiple tissues. A key feature of our approach is that it only requires single SNP p -values and their minor allele frequencies (MAFs), or estimated allelic effect and standard error, combined with closed form analytical results that enable quick comparisons, even at the genome-wide scale. Our Bayesian procedure provides intuitive posterior probabilities that can be easily interpreted. A main application of our method is the systematic comparison between a new GWAS dataset and a large catalogue of association studies in order to identify novel shared mechanisms. We demonstrate the value of the method by re-analysing a large scale meta-analysis of blood lipids [1] in combination with a gene expression study in 966 liver samples [14].

Results

Overview of the method

We consider a situation where two traits (denoted by Y_1, Y_2) have been measured in two distinct datasets of unrelated individuals. We assume that samples are drawn from the same ethnic group, i.e. allele frequencies and pattern of linkage disequilibrium (LD) are identical in both populations. We consider, for each variant, a linear trend model between the outcome phenotype Y and the genotypes X (or a log-odds generalised linear model if one of the two outcome phenotypes Y is binary):

$$Y = \mu + \beta X + \epsilon$$

We are interested in a situation where single variant association p -values and MAFs, or estimated regression coefficients $\hat{\beta}$ and their estimated precisions $var(\hat{\beta})$, are available for both datasets at Q variants, typically SNPs but also indels. We make two additional assumptions and discuss later in this paper how these can be relaxed. Firstly, that the causal variant is included in the set of Q variants, either directly typed or well imputed [15–17]. Secondly, that at most one association is present for each trait in the genomic region of interest. We are interested in exploring whether the data support a shared causal variant for both traits. While the method is fully applicable to case-control outcome, we consider two quantitative traits in this initial description.

SNP causality in a region of Q variants can be summarised for each trait using a vector of length Q of $(0, 1)$ values, where 1 means that the variant is causally associated with the trait of interest and at most one entry is non-zero. A schematic illustration of this framework is provided in Figure 1 in a region that contains 8 SNPs. Each possible pair of vectors (for traits 1 and 2, which we refer to as “configuration”) can be assigned to one of five hypothesis:

- \mathbb{H}_0 : No association with either trait

- \mathbb{H}_1 : Association with trait 1, not with trait 2
- \mathbb{H}_2 : Association with trait 2, not with trait 1
- \mathbb{H}_3 : Association with trait 1 and trait 2, two independent SNPs
- \mathbb{H}_4 : Association with trait 1 and trait 2, one shared SNP

In this framework, the colocalisation problem can be re-formulated as assessing the support for all configurations (i.e. pairs of binary vectors) in hypothesis \mathbb{H}_4 .

Our method is Bayesian in the sense that it integrates over all possible configurations. This process requires the definition of prior probabilities which are defined at the SNP level (Methods). A likelihood can be assigned to each configuration, and these likelihoods can be summed over all configurations and combined with the prior to assess the support for each hypotheses (\mathbb{H})₁⁵. The result of this procedure is five posterior probabilities (PP0, PP1, PP2, PP3 and PP4). A large posterior probability for hypothesis 3, PP3, indicates support for two independent causal SNPs associated with each trait. In contrast, if PP4 is large, the data support a single variant affecting both traits. An illustration of the method is shown in Figure 2 for negative (Fig 2A-B, *FRK* gene and LDL, PP3 > 90%) and positive (Fig 2C-D, *SDC1* gene and total cholesterol, PP4 > 80%) colocalisation results.

While the method uses Approximate Bayes Factor computations (ABF, [18], and Methods), no iterative computation scheme (such as Markov Chain Monte Carlo) is required. Therefore, computations are quick and do not require any specific computing infrastructure. Precisely, the computation time behaves as Q^d , where Q is the number of variants in the genomic region and d the number distinct associations (typically $d = 2$, assuming two traits and at most one causal variant per trait). For all applications considered here, the computation time is nearly instant. Importantly, the use of ABF enable the computation of posterior probabilities from single variant association p -values and MAFs, although the estimated single SNP regression coefficients $\hat{\beta}$ and their variances or standard errors are preferred for imputed data.

Sample size required for colocalisation analysis

Given the well understood requirements for large sample size for GWAS data, we used simulations to investigate the power of our approach. We generated pairs of eQTL/biomarker datasets assuming a shared causal variant. We varied two parameters: the sample size of the biomarker dataset and the proportion of the biomarker variance explained by the shared genetic variant. We set the proportion of the eQTL variance explained by the shared variant to 10% and we used the original sample size of the liver eQTL dataset described herein [14]. Results are shown in Figure 3. We find that given a sample size of 2,000 individuals for the biomarker dataset, the causal variant needs to explain close to 2% of the variance of the biomarker to provide reliable evidence in favour of a colocalised signal (lower 10th percentile for PP4 > 80%).

Consequence of limited variant density

Until recently the assumption that, for a given GWAS signal, the causal variant in that interval had been genotyped was unrealistic. However, the application of imputation techniques [15–17] can provide genotype information about the majority of common genetic variants. Therefore, in situations where a common variant drives the GWAS signal, it is now plausible that, in imputed datasets, genotype information about this variant is available. Nevertheless, limited imputation quality can invalidate this hypothesis. This prompted us to investigate the implication of not including the causal variant in the genotype panel.

To address this question, we used Illumina MetaboChip data and imputed the genotyped regions using the Minimac software ([17] and Methods). We then selected only the subset of variants present in the Illumina 660K genotyping array. We simulated data under the assumption of a shared causal variant, with 4,000 individuals in the biomarker dataset. We then computed the PP4 statistic with and without restricting the SNP set to the Illumina 660K Chip SNPs (Figure 4). We also considered two different scenarios, with the causal SNP included/not included in the Illumina 660W panel (Figure ?? and Figure ?? for more exhaustive simulations).

Our results show that when the causal variant is directly genotyped by the low density array, the use of imputed data is not essential (Figure 4A). However, in cases where the causal variant is not typed or imputed in the low density panel, the variance of PP4 is much higher (Figure 4B). In this situation, the resulting PP4 statistic tends to decrease even though considerable variability is observed. Inspection of simulation results in Figure 5 (bottom row for tagging SNP, leftmost graph for shared causal variant) shows that while PP4 tends to be lower than for its counterpart with complete genotype data (top row, leftmost graph), PP3 remains low. This indicates that more probability is given to PP0, PP1 and PP2, which can be interpreted as a loss of power rather than misleading inference in favour of distinct variants for both traits.

Comparison with existing colocalisation tests

We compared the behaviour of our proposed test with that of proportional colocalisation testing [11, 13] in the specific case of a biomarker dataset with 10,000 samples (Figure 5). Broadly, in the case of either a single common causal variant or two distinct causal variants, our proposed method could infer the simulated hypotheses correctly (PP4 or PP3 > 0.9) with good confidence, and PP3 > 0.9 slightly more often than the proportional testing p -value < 0.05. A key advantage in our Bayesian approach is the ability to distinguish evidence for colocalisation (i.e. high PP4) from a lack of power (i.e. high PP0, PP1 or PP2). In both of these cases (high PP4 or high PP0/PP1/PP2), the use of the proportional approach leads to failure to reject the null even though the interpretation of these situations should differ.

It has been proposed that gene expression may be subject to both global regulatory variation which acts across multiple tissues and secondary tissue specific regulators [19]. Neither approach covers this case explicitly in its construction, but it is instructive to examine their expected behaviour. The proportional approach tends to reject a null of colocalisation, suggesting that a single distinct causal variant can be sufficient to violate the null hypothesis of proportional regression coefficients. In contrast, the Bayesian approach tends to favour the shared variant in the cases covered by our simulations (median PP4 > median PP3), and either hypotheses H3 or H4 can potentially have strong support (PP4 > 0.9 in close to 50% of simulations, and PP3 > 0.9 in around 25% of simulations). Of course, the ultimate goal should be to extend these tests to cover multiple causal variants, but in the meantime, it can be useful to know that a high PP4 in our proposed Bayesian analysis indicates strong support for “at least one causal variant” and that rejection of the null of proportionality of regression coefficients indicates that the two traits do not share all causal variants, not that they cannot share one.

Dealing with several independent associations for the same trait

We have so far assumed that each trait is associated with at most one causal variant per locus. However, recent studies have shown that it is not unusual to observe two or more independent associations at a locus for a trait of interest [20]. The natural and statistically exact modification of our approach would compute, for each trait, Bayes factors for sets of SNPs rather than single SNPs (up to n SNPs jointly to accommodate for n distinct associations per trait). However, this approach has two drawbacks. Firstly, the interpretation of the resulting posterior probabilities is more challenging in situations where some but not all of the variants are shared across both traits. More importantly, the typical approach consists of

publishing single variant summary statistics, which would prevent the use of standard summary statistics, a key feature of our approach.

An alternative approach to account for multiple associations is motivated by the fact that, when distinct associations for the same trait are present at a locus, the assumption of a single variant per trait prompts the algorithm to consider only the strongest of these distinct association signals. Secondary signals, including potential rare variant associations yielding marginal P-values, have little to no impact on the resulting posterior probabilities. Therefore, a stepwise strategy successively conditioning on the top SNP to reveal the secondary association signals, can be an effective approximation. In situations where only single SNP summary statistics are available, the approximate conditional meta-analysis framework proposed by Visscher et al [21] can be used to obtain conditional p -values. Another consequence of the behaviour of our inference procedure when the single causal variant assumption is enforced is that the posterior probabilities can be affected by the presence of two independent associations at the same locus with similar levels of significance.

Application to a meta-analysis of blood lipids combined with a liver expression dataset

Teslovich et al. [1] reported common variants associated with plasma concentrations of low-density lipoprotein cholesterol (LDL), high-density lipoprotein cholesterol (HDL) and triglyceride (TG) levels in more than 100,000 individuals of European ancestry. They then reported the correlations between the lead SNPs at the loci they found and the expression levels of transcripts in liver. For the lipid dataset we have access only to summary statistics. The liver expression dataset used in this analyses is the same as the one used in Teslovich et al. Teslovich et al. defined a region within 500 kilobases of the lead SNP, and the threshold for significance is 10^{-8} . At this threshold, they found 38 SNP-to-gene eQTLs in liver (Supplementary Table 8 of [1]). Table S1 shows our results for these 38 previously reported colocalisations. A complete list of all our identified colocalisations (independently of previous reports) is provided in Tables S2, S3, S4, S5 (broken down by lipid trait).

The majority of our results are consistent the findings of Teslovich et al (Table S1). However, Table 1 lists the previously reported lipid-eQTL for which we find strong support *against* the colocalisation hypothesis (PP3 > 75%). To assess the role of the prior, we varied the critical parameter p_{12} , which codes for the prior probability that a variant is associated with both traits. Here we report the results using the $p_{12} = 10^{-6}$. The complete list of results is provided in Table ???. We found six potential “false positive” lipid-eQTL pairs for which our analysis does not support a colocalisation reported in Teslovich et al (Table 1). In addition, we found strong evidence of distinct signals between *HLA-DQ/HLA-DR* and TC (Table S1) but these results must be interpreted with caution owing to the extensive polymorphism in the major histocompatibility complex region. Furthermore, the evidence for *TMEM50A* expression and LDL (PP3 = 58%) or TC (PP3 = 60%) is not strong enough to support either models (Table S1), so we cannot make a firm statement in this case. In one case, *CEP250*, our re-analysis of the expression data did not identify an eQTL for this gene. In such a situation, both PP3 and PP4 are low and PP0, PP1 and PP2 concentrate most of the posterior distribution.

Table 2 lists the 14 colocalised loci (15 genes) that were not reported by Teslovich et al (or in Global Lipids Genetics Consortium [22] for the gene *NYNRIN*), but for which our method finds strong support for colocalisation (PP4 > 75%). Figure S6 shows the locuszoom plots for these colocalisation results. Eleven of these 15 genes are strong candidates for involvement in lipid metabolism and/or have been previously suggested as candidate genes: *SDC1*, *TGOLN2*, *INHBB*, *UBXN2B*, *VLDLR*, *VIM*, *CYP26A1*, *OGFOD1*, *HP*, *HPR*, *PPARA*. See supplemental for a brief overview of the function of these genes. Four others genes have a less obvious link: *CMTM6*, *C6orf106*, *CUX2*, *ENSG00000259359*.

Three previously reported genes (*SYPL2*, *IFT172*, *TBKBP1*) which, based on our re-analysis, do not colocalise with the lipid traits, have a nearby gene with a high probability of colocalisation (resp. *SORT1*,

GCKR, *KPNB1*). This suggests that these genes are more likely candidates in this region. To explore the possibility that secondary signals may colocalise, we applied the stepwise regression strategy described above to deal with several independent associations at a single locus. We performed colocalisation test using eQTL results conditional on the top eQTL associated variant. Two of the loci (*SYPL2*/LDL or TC, *APOC4* and TG) showed evidence of colocalisation with expression after conditional analysis (Table 1).

An example of this stepwise procedure for the gene *SYPL2* and LDL is provided in Figure 6. We find that the top liver eQTL signal is clearly discordant with LDL association (Table 1 and Figure 6). However, conditioning on the top eQTL signal reveals a second independent association for *SYPL2* expression in liver. This secondary *SYPL2* eQTL colocalises with the LDL association (PP4 > 90%, Figure 6).

Web based resource

We developed a web site designed for integration of GWAS results using only p -values and the sample size of the datasets (<http://coloc.cs.ucl.ac.uk/coloc/>). The website was developed using RWUI [23]. Results include a list of potentially causal genes with the associated PP4 with their respective plots and ABF, and can be viewed either interactively or returned by email.

Researchers can request a genome-wide scan of results from a genetic association analysis, and obtain a list of genes with a high probability of mediating the GWAS signals in a particular tissue. The tools also allows visualisation of the signals within a genetic region of interest.

The database and browser currently include the possibility of investigating colocalisation with liver [1] and brain [24, 25] expression data, however the resource will soon be extended to include expression in different tissues. This method, as well as alternative approaches for colocalisation testing [11, 13], are also available with additional input options in an R package, *coloc*, from the Comprehensive R Archive Network (<http://cran.rproject.org/web/packages/coloc>).

Discussion

We have developed a novel Bayesian statistical procedure to assess whether two association signals are colocalised. The strength of this approach lies in its speed and analytical forms, combined with the fact that it can use single variant p -values when only these are available. Our method differs from a typical fine-mapping exercise in the sense that we are not interested in knowing which variant is likely to be causal but only whether a shared causal variant is plausible.

Our results show that to provide an accurate answer to the colocalisation problem, high density genotyping and/or accurate use of imputation techniques are key. The quality of the imputation is another important parameter. Indeed, while the variance of the regression coefficient can be estimated solely on the basis of the minor allele frequency for typed SNPs and sample size (and the case control ratio in the case of a binary outcome) [15, 26], this ignores the uncertainty due to imputation. Filtering out poorly imputed SNPs partially addresses this problem, with the drawback that it may exclude the causal variant(s). Hence, providing estimates of the variance of the MLE, together with the effect estimates, will result in greater accuracy. This additional option is available on the *coloc* package in R (<http://cran.rproject.org/web/packages/coloc>).

We currently assume that each genetic variant is equally likely a priori to affect gene expression or trait. A straightforward addition to our methodology would consider location specific priors for each variant, which would depend for example on the distance to the gene of interest, or the presence of functional elements in this chromosome region [27, 28]. Our computation of the BF also assumes that, under \mathbb{H}_4 , the effect sizes of the shared variant on both traits are independent. This could be modified if, for example, one compares eQTLs across different tissue types, or the same trait in two different studies. [29] has proposed

a framework to deal with correlated effect sizes, and these ideas could potentially be incorporated in our colocalisation test.

Another prior related issue is the choice of prior probabilities for the various configurations. For the eQTL analysis, we used a 10^{-4} prior probability for a cis-eQTL. A more stringent threshold may be better suited for trans-eQTLs where the variants are further away from the gene under genetic control. We also used a prior probability of 10^{-4} for the lipid associations. Although our knowledge about this is still lacking, this estimate has been suggested in the literature in the context of GWAS [18, 30, 31]. We assigned a prior probability of 1×10^{-6} for p_{12} , which encodes the probability that a variant affects both traits. It has been shown that SNPs associated with complex traits are more likely to be eQTLs compared to other SNPs chosen at random from GWAS platforms [32], and a higher weighting for these SNPs has been proposed when performing Bayesian association analyses [33, 34]. Also, eQTLs have been shown to be enriched for disease-associated SNPs when a disease-relevant tissue is used [8, 35]. Our sensitivity analysis for the p_{12} parameter showed broadly consistent results (Table S1). In cases where GWAS data are available for both traits, [9] show that it is possible to estimate these parameters from the data using a hierarchical model. This addition is a possible extension of our approach.

The interpretation of the posterior probabilities requires caution. For example, a low PP4 may not indicate evidence against colocalisation in situations where PP3 is also low. It may simply be the result of limited power, which is evidenced by high values of PP0, PP1 and/or PP2. Moreover, a high PP4 is a measure of correlation, not causality. To illustrate this, one can consider the relatively common situation where a single variant appears to affect the expression of several genes in a chromosome region (as observed, for example, in the region surrounding the *SORT1* gene). Several eQTLs will be colocalised, both between them and with the biomarker of interest. In this situation one would typically expect that a single gene is causally involved in the biomarker pathway but the colocalisation test with the biomarker will generate high PP4 values for all genes in the interval.

We show that we can use conditional p -values to deal with multiple independent associations with the same trait at one locus. While we found this solution generally effective, Wallace [13] points out that this top SNP selection for the conditional analysis can create biases, although the bias is small in the case of large samples and/or strong effects. For difficult loci with multiple associations for both traits and available genotype data, it may be more appropriate to estimate Bayes factors for sets rather than single variants in order to obtain an exact answer. This extension would avoid the issue of SNP selection for the conditional analysis.

Importantly, GWAS signals can be explained by eQTLs only when the causal variant affects the phenotype by altering the amount of mRNA produced, but not when the phenotype is affected by changing the type of protein produced, although the former seems to be the most common [32]. Furthermore, since many diseases manifest their phenotype in certain tissues exclusively [3, 19, 36, 37], colocalisation results will be dependent on the expression dataset used. In addition to identifying the causal genes, the identification of tissue specificity for the molecular effects underlying GWAS signals is a key outcome of our method. We anticipate that building a reference set of eQTL studies in multiple tissues will provide a useful check for every new GWAS dataset, pointing directly to potential candidate genes/tissue types where these effects are mediated.

While this report focuses on finding shared signals between a biomarker dataset and a liver expression dataset, we plan to utilise summary results of multiple GWAS and eQTL studies, for a variety of cell types and traits. In fact, our method can utilise summary results from any association studies. Disease/disease, (*cis* or *trans*) eQTL/disease or disease/biomarkers comparisons are all of biological interest and use the same statistical framework. We expect that the fact that the test can be based on single SNP summary statistics will be key to overcome data sharing concerns, hence enabling a large scale implementation of this tool. The increasing availability of RNA-Seq eQTL studies will further increase the opportunity to detect isoform specific eQTLs and their relevance to disease studies. Owing to the increasing availability of GWAS datasets, the systematic application of this approach will potentially provide clues into the

molecular mechanisms underlying GWAS signals and the aetiology of the disorders.

Materials and Methods

Expression dataset

We used in our analysis gene expression and genotype data from 966 human liver samples. The samples were collected post-mortem or during surgical resection from unrelated European-American subjects from two different non-overlapping studies, which have been described in [14]. The cohorts were both genotyped using Illumina 650Y BeadChip array, and 39,000 expression probes were profiled using Agilent human gene expression arrays. All of the expression data has been normalised as one unit even though they were part of different studies, since high concordance between data generated using the same array platforms has been previously reported. Probe sequences were searched against the human reference genome GRCh37 from 1000genomes using BLASTN. Multiple probes mapping to one gene were kept in order to examine possible splicing. The probes were kept and annotated to a specific gene if they were entirely included in genes defined by Ensembl ID or by HGNC symbol using the package `biomaRt` in R [38]. After mapping and annotating the probes, we were left with 40,548 mapped probes covering 24,927 genes.

Imputation of genetic data

Quality control filters were applied both before and after imputation. Before imputation, individuals with more than 10% missing genotypes were removed, and SNPs showing a missing rate greater than 10%, a deviation for HWE at a p -value less than 0.001 were dropped. After imputation, monomorphic SNPs were excluded from analyses.

To speed up the imputation process, the genome was broken into small chunks that were phased and imputed separately and then re-assembled. This was achieved using the `ChunkChromosome` tool (<http://genome.sph.umich.edu/wiki/ChunkChromosome>), and specifying chunks of 1000 SNPs, with an overlap window of 200 SNPs on each side, which improves accuracy near the edges during the phasing step. Each chunk was phased using the program `MACH1` (Versions 1.0.18, downloaded from: <http://www.sph.umich.edu/csg/abecasis/MACH/download/>) with the number of states set to 300 and the number of rounds of MCMC set to 20 for all chunks. Phased haplotypes were used as a basis for imputation of untyped SNPs using the program `Minimac` (version 2011.10.27, downloaded from: <http://www.sph.umich.edu/csg/cfuchsb/minimac-beta-2012.8.15.tgz>) with 1000 Genomes EUR reference haplotypes (phase1 version 3, March 2012) to impute SNPs not genotyped on the Illumina array. The data was then collated in probability format that can be used by the R Package `snpStats` [38].

eQTL analysis

eQTL p -values, effect sizes, and standard errors were obtained by fitting a linear trend test regression between the expression of each gene and all variants 200 kilobases upstream and downstream from each probe. After filtering out the variants with $MAF < 0.001$, monomorphic SNPs, multi-allelic SNPs (as reported in 1000 Genomes or in the Ensembl database) and variants not sufficiently well imputed ($Rsq < 0.3$, as defined by `minimac` <http://genome.sph.umich.edu/wiki/minimac>) between both datasets, we applied our colocalisation procedure. We conducted conditional analysis on SNPs with p -values $< 10^{-4}$ for the expression associations, and repeated the colocalisation test using expression data conditioned on the most significant SNP. The aim of this analysis is to explore whether additional signals for expression other than the main one are shared with the biomarker signal.

Biomarker dataset

The biomarker p -values from the meta-analyses (with genomic control correction) were obtained from a publicly available repository (<http://www.sph.umich.edu/csg/abecasis/public/lipids2010/>).

Posterior Computation

We call a “configuration” one possible combination of pairs of binary vectors indicating whether the variant is associated with the selected trait. We can group the configurations into five sets, S_0, S_1, S_2, S_3, S_4 , containing assignments of all SNPs Q to the functional role corresponding to the five hypothesis $\mathbb{H}_0, \mathbb{H}_1, \mathbb{H}_2, \mathbb{H}_3, \mathbb{H}_4$. We can compute the posterior probabilities for each of these 5 hypothesis using a Bayesian approach. Firstly, we calculate the likelihood of each hypothesis,

$$L(H_h) = L(H_h | D) = \sum_{S \in S_h} P(D | S)P(S) \quad (1)$$

where $P(S)$ is the prior probability of a configuration, $P(D | S)$ is the probability of the observed data D under a given configuration (which we will refer to as the likelihood of this configuration), and the sum is over all configurations S which are consistent with a given hypothesis H_h , $h=(1,2,3,4)$. Thus, each configuration likelihood is weighted by the prior probability of that configuration.

Next, we compute the posterior probability by taking the ratio of the hypothesis likelihoods under the different hypotheses. For example, the posterior probability under hypothesis 4 is:

$$PP4 = \frac{L(H_4)}{L(H_0) + L(H_1) + L(H_2) + L(H_3) + L(H_4)} \quad (2)$$

If we also divide each probability by the baseline $L(H_0)$ we get:

$$PP4 = \frac{\frac{L(H_4)}{L(H_0)}}{1 + \frac{L(H_1)}{L(H_0)} + \frac{L(H_2)}{L(H_0)} + \frac{L(H_3)}{L(H_0)} + \frac{L(H_4)}{L(H_0)}} \quad (3)$$

The ratios in the numerator and denominator of equation 3 are:

$$\frac{L(H_h)}{L(H_0)} = \sum_{S \in S_h} \frac{P(D | S)}{P(D | S_0)} \times \frac{P(S)}{P(S_0)} \quad (4)$$

The first ratio in this equation is a Bayes Factor (BF) for each configuration, and the second ratio is the prior odds of a configuration compared with the baseline configuration S_0 . The BF can be computed for each variant from the p -value, or estimated regression coefficient $\hat{\beta}$ and variance of $\hat{\beta}$, using Wakefield’s method. By summing over all configurations in S_h we are effectively comparing the support in the data for one alternative hypothesis versus the null hypothesis.

Bayes factor computation

A Bayes Factor for each SNP and each trait 1 and 2 was computed using the Approximate Bayes Factor (ABF, [18]). Wakefield’s method yields a Bayes factor that measures relative support for a model in which the SNP is associated with the trait compared to the null model of no association.

The equation used is the following:

$$ABF = \frac{1}{\sqrt{1-r}} \times \exp \left[-\frac{Z^2}{2} \times r \right] \quad (5)$$

where $Z = \hat{\beta}/\sqrt{V}$ is the usual Z statistic and the shrinkage factor r is the ratio of the variance of the prior and total variance ($r = W/(V + W)$).

Assuming a normal distribution, the p -value of each SNP can be converted to standard one-tailed Z-score by using inverse normal cumulative distribution function. So for a SNP, all that is needed are the p -values from a standard regression output, and \sqrt{W} , the standard deviation of the normal prior $N(0, W)$ on β .

The variance of the effect estimate, V , can be approximated using the MAF and sample size. However for imputed data it is preferable to use the variance outputted in standard regression analysis directly in the ABF equation. For the expression dataset used here, the variance and effect estimates from the regression analysis were used for computation of ABFs. More details can be found in the Supplementary materials.

Choice of priors

Prior probabilities are assigned at the SNP level and correspond to mutually exclusive events. We assigned a prior of 1×10^{-4} for p_1 and p_2 , the probability that a SNP is associated with either of the two traits. Since all SNPs are assumed to have the same prior probability of association, this prior can be interpreted as an estimate for the proportion of SNPs that we expect to be associated with the trait in question.

We also assigned a prior probability of 1×10^{-6} for p_{12} , the probability that one SNP is associated with both traits. This probability can be better understood when it is re-expressed as the conditional probability of a SNP being associated with trait 2, given that it is associated with trait 1. So assigning a probability of 1×10^{-6} means that 1 in 100 SNPs that are associated with trait 1 is also associated with the other. As a sensitivity analysis, we ran the comparison with Teslovich et al. using two other prior probabilities for p_{12} , $p_{12} = 2 \times 10^{-6}$ which means 1 in 50 SNPs that are associated with one trait is also associated with the other; and $p_{12} = 10^{-5}$ which means 1 in 10 SNPs.

To compute the ABF, we also needed to specify the standard deviation for the prior, and we set this to 0.20 for binary traits and 0.15 for quantitative traits (more details in Supplementary).

Acknowledgments

Claudia Giambartolomei is supported by a grant from the British Heart Foundation (CD6H).

The Diabetes and Inflammation Laboratory is funded by the JDRF, the Wellcome Trust (091157) and the National Institute for Health Research (NIHR) Cambridge Biomedical Research Centre. The Cambridge Institute for Medical Research (CIMR) is in receipt of a Wellcome Trust Strategic Award (100140).

Figures

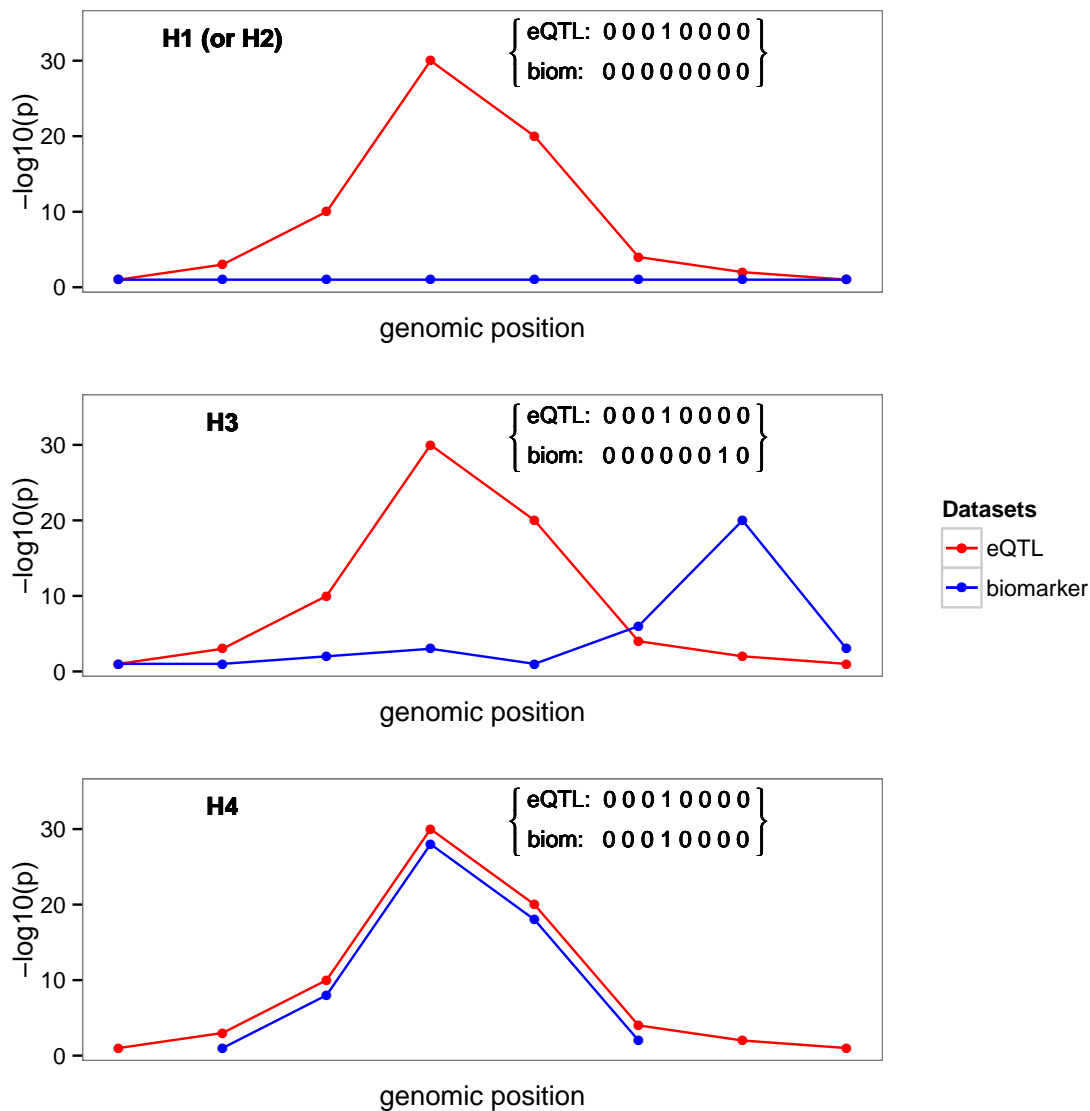


Figure 1. Example of one configuration under different hypotheses represented by one binary vector for each trait of $(0, 1)$ values of length $n = 8$, the number of shared variants in a region. The value of 1 means that the variant is causally involved in disease, 0 that it is not. The first plot shows the case where only one dataset shows an association. The second plot shows that the causal SNP is different for the biomarker dataset compared to the expression dataset. The third plot shows the configuration where the single causal variant is the fourth one.

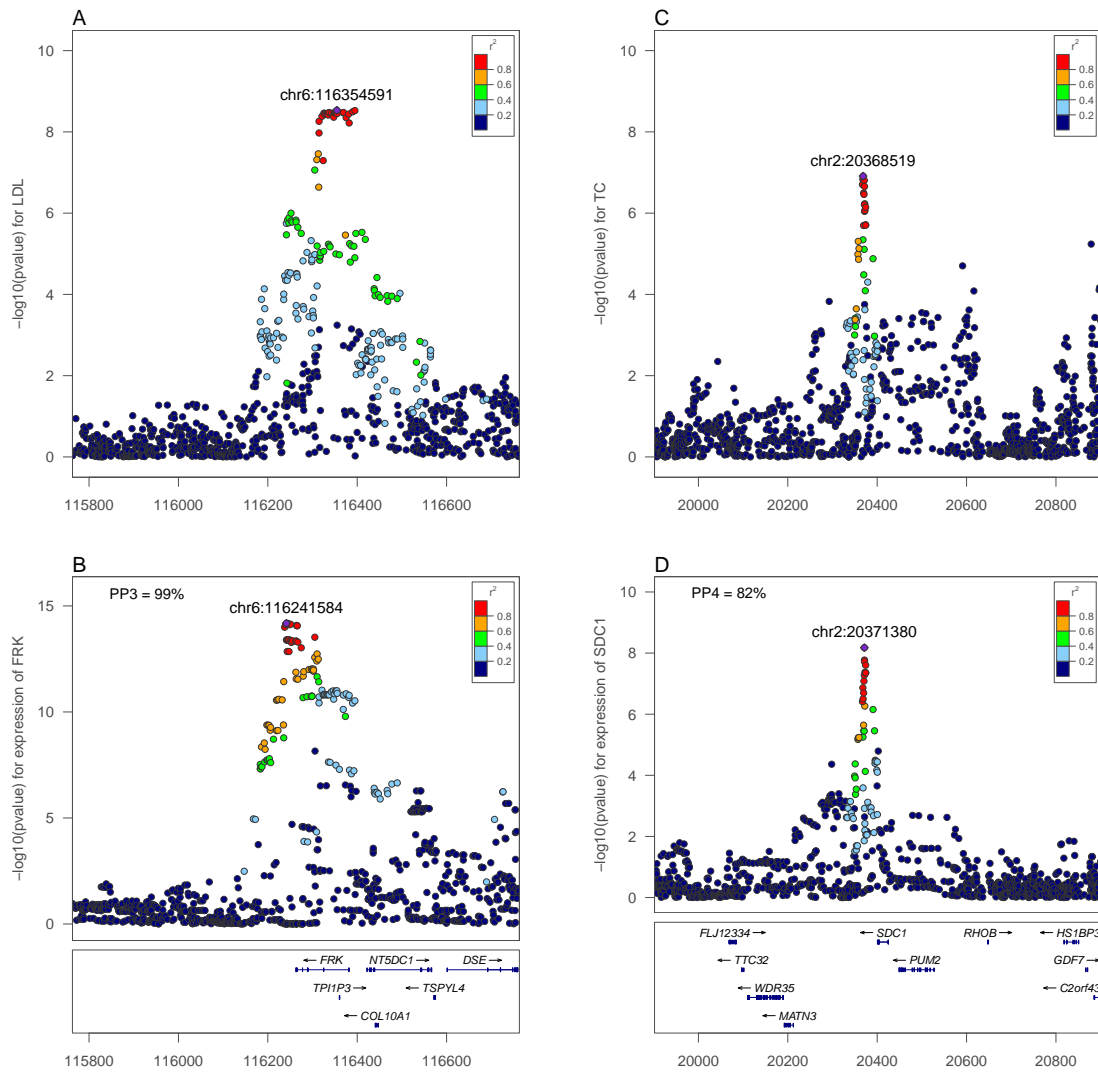


Figure 2. Illustration of the colocalisation results. Negative(A-B, FRK gene and LDL, PP3 > 90%) and positive (C-D, SDC1 gene and total cholesterol, PP4 > 80%) colocalisation results. $-\log_{10}(\text{p})$ association p -values for biomarker (top, A and C) and $-\log_{10}(\text{p})$ association p -values for expression (bottom, B and D) at the *FRK* (A, B) and *SDC1* locus (C, D), 1Mb range.

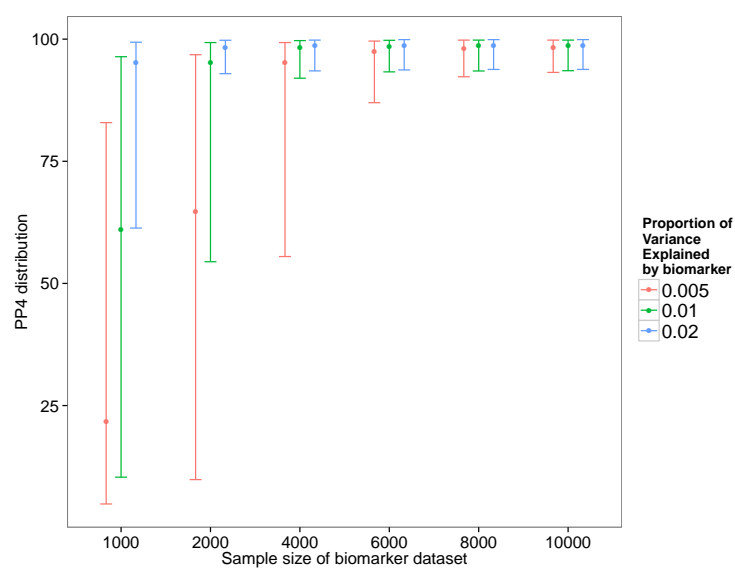


Figure 3. Simulation analysis with a shared causal variant between two studies: one eQTL (sample size 966 samples, 10% of the variance explained by the variant) and one biomarker (such as LDL). The variance explained by the biomarker is colour coded and the x-axis shows the sample size of the biomarker study. The y axis shows the median, 10% and 90% quantile of the distribution of PP4 values (which supports a shared common variant).

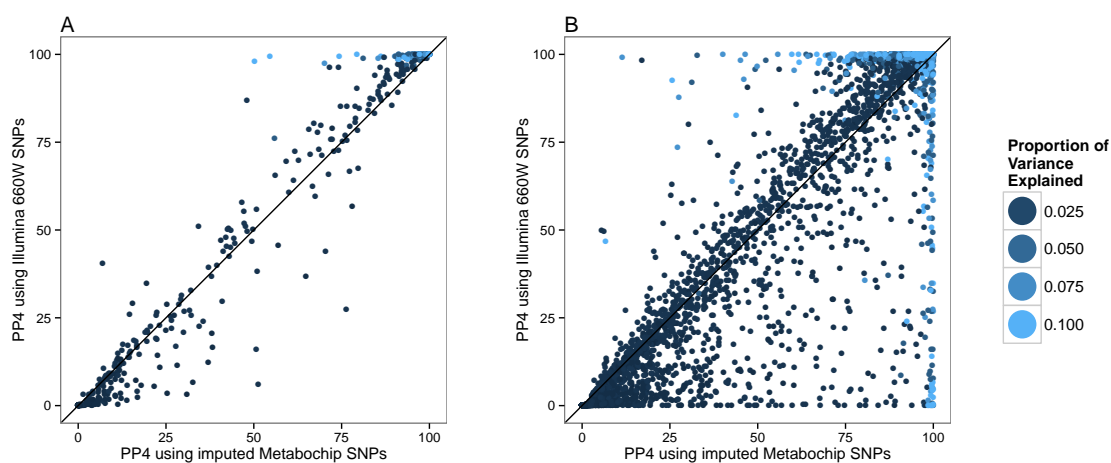


Figure 4. Simulation analysis with a shared causal variant between two studies: one eQTL (sample size 966 samples) and one biomarker (sample size of 4,000 samples). The variance explained by the biomarker and the expression is the same and is colour coded. The x-axis shows the estimated PP4 for 1,000 simulations using data imputed from metaboChip Illumina array. The y-axis uses the same dataset restricted to variants present on the Illumina 660W genotyping array to assess the impact of a lower variant density. **A.** The causal variant is included in the Illumina 660W panel. **B.** The causal SNP not included in Illumina 660W panel.

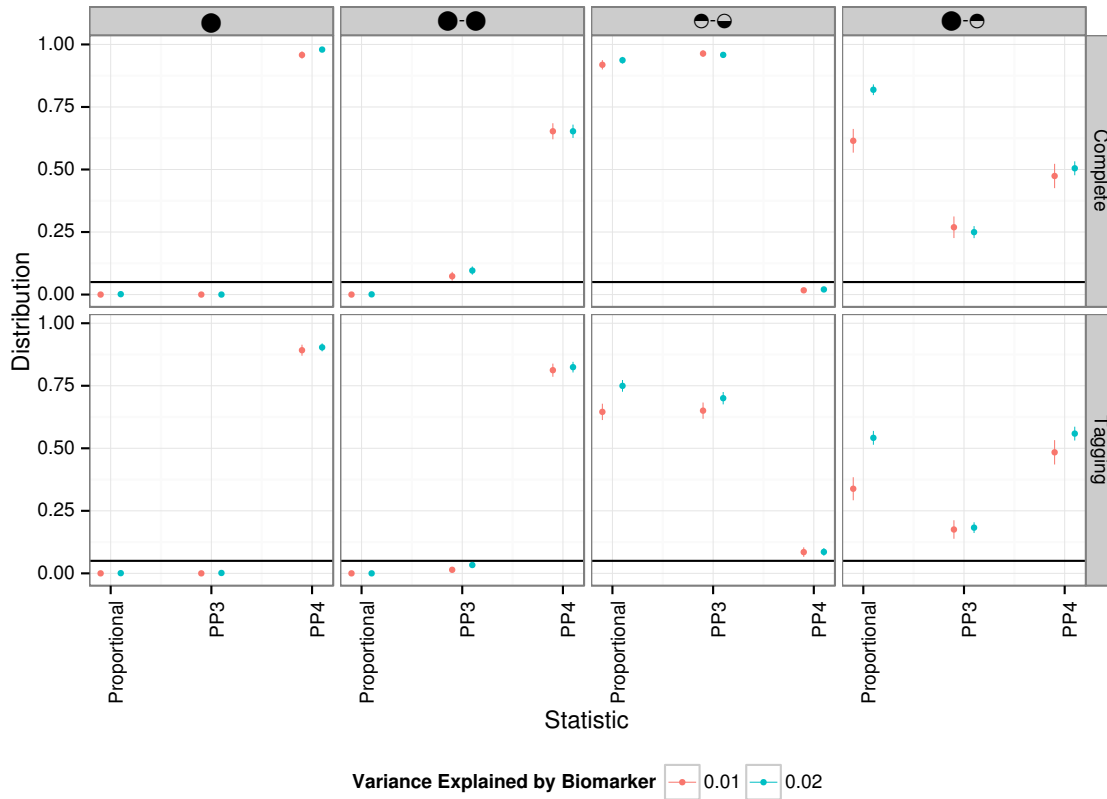


Figure 5. Summary of proportional and Bayesian colocalisation analysis of simulated data.

Each plot shows a different scenario, the total number of causal variants in a region is indicated by number of circles in the plot titles with causal variants affecting both traits, the eQTL trait only, or the biomarker trait only, indicated by full circles, top-shaded circles and bottom-shaded circles respectively. In the top row the causal variant is typed or imputed, whereas only tag variants are typed/imputed in the bottom row. For proportional testing (under the BMA approach), we show the proportion of simulations with posterior predictive P-value $p < 0.05$ (black horizontal line) while for our Bayesian analysis we plot the proportion of simulations with the posterior probability (PP3 or PP4) of the indicated hypothesis > 0.9 . Error bars show 95% confidence intervals (estimated based on an average of 1,000 simulations per scenario). In all cases, for the eQTL sample size is 1,000; genetic variants explain a total of 10% of eQTL variance; for the biomarker trait, the sample size is 10,000.

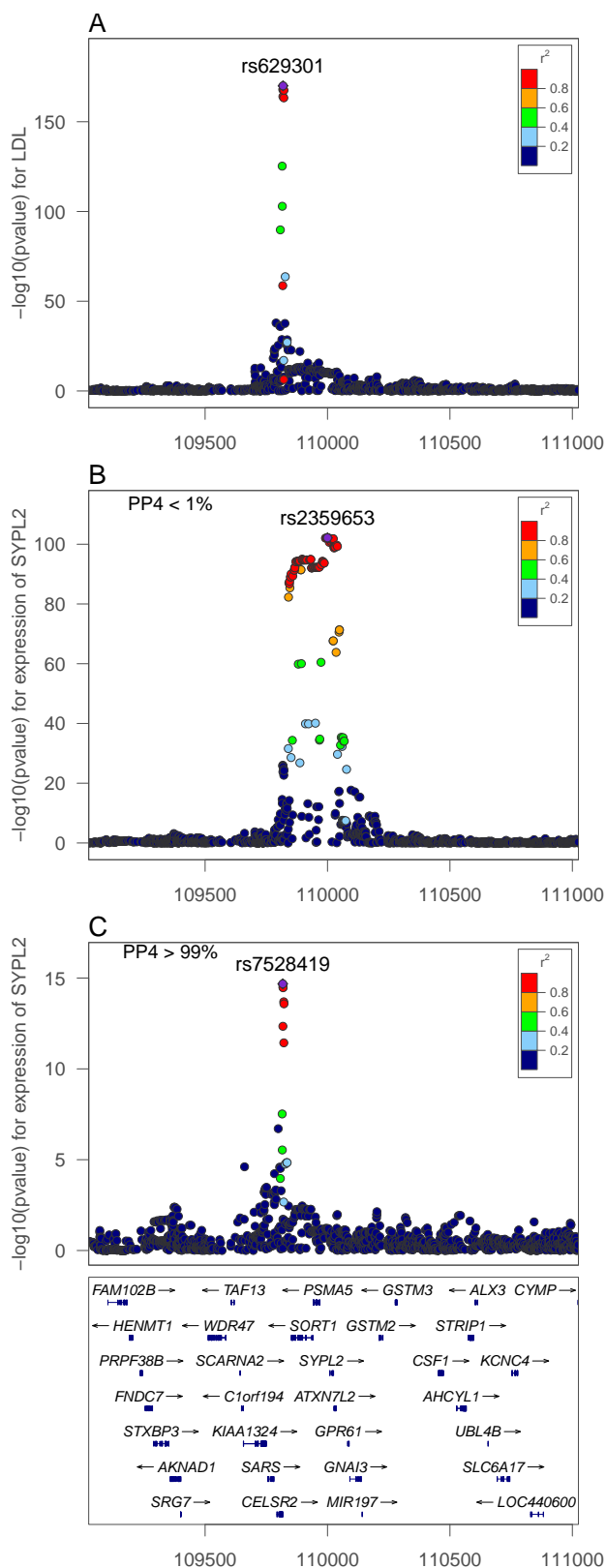


Figure 6. LDL association and eQTL association plots at the *SYPL2* locus. The x-axis shows the physical position on the chromosome (Mb) **A**: $-\log_{10}(p)$ association p -values for LDL. The p -values are from the Teslovich et al published meta-analysis of > 100,000 individuals. **B**: $-\log_{10}(p)$ association p -values for *SYPL2* expression in 966 liver samples. **C**: $-\log_{10}(p)$ association p -values for *SYPL2* expression conditional on the top eQTL associated SNP at this locus (rs2359653).

Tables

Table 1. Loci previously reported to colocalise with liver eQTL, but not supported by our analysis

Chr	Region	Gene	Trait	Biom pval	Biom SNP	eQTL pval	eQTL SNP	Primary signal		Secondary signal*		Other genes colocalising in region (PP4 > 75%)
								PP3 (%)	PP4 (%)	PP4 (%)	conditional SNP	
1	109824678:110224737	<i>SYPL2</i>	LDL	9.7e-171	rs629301	7.1e-103	rs2359653	> 99	< 1	99	rs2359653	<i>SORT1/CELSR2/PSRC1/PSMA5</i> <i>SORT1/CELSR2/PSRC1/PSMA5</i>
			TC	8.0e-52	rs672569	7.1e-103	rs2359653	> 99	< 1	99	rs2359653	
2	27467244:27867303	<i>IFT172</i>	TG	5.7e-133	rs1260326	1.7e-130	rs704791	> 99	< 1			<i>C2orf16/GCKR</i> <i>C2orf16/GCKR</i>
			TC	7.3e-27	rs1260326	1.7e-130	rs704791	> 99	< 1			
6	116062804:116462863	<i>FRK</i>	LDL	2.9e-09	rs11153594	6.6e-15	rs195517	99	1			
			TC	1.7e-10	rs9488822	6.6e-15	rs195517	94	6			
17	45589357:45989416	<i>TBKBP1</i>	LDL	1.1e-07	rs8072100	2.1e-21	rs9913503	87	9			<i>KPNB1</i> <i>KPNB1</i>
			TC	1.8e-07	rs8072100	2.1e-21	rs9913503	92	2			
19	45248464:45648523	<i>APOC1</i>	TG	1.1e-30	rs439401	1.1e-299	19:45452692:A_AG	> 99	< 1	96	19:45452692:A_AG	
20	34013995:34414054	<i>CPNE1</i>	TC	3.8e-10	rs2277862	7.3e-110	rs6060524	> 99	< 1			

Gene/eQTL associations previously reported as having a probable shared variant but not supported by our method based on PP3 (posterior probability for distinct signal values) > 75%. *Secondary signals are reported only when there is a secondary eQTL at a p -value greater than 10^{-4} . Colocalisation tests are computed using the expression data conditioned on the listed SNP. Other genes in the same region as the gene listed that colocalise using our method are reported.

Table 2. Novel loci not previously reported to colocalise with liver eQTL, but colocalising based on our analysis

Chr	Region	Gene	Trait	PP.H3.abf	PP.H4.abf	Reference
2	20201795:20601854	<i>SDC1</i>	TC	17	82	[39]
2	85349026:85749085	<i>TGOLN2</i>	HDL	17	83	[40]
2	120908798:121308857	<i>INHBB</i>	LDL	7	77	[41]
3	32322873:32722932	<i>CMTM6</i>	TC	8	77	
6	34355095:34755154	<i>C6orf106</i>	TC	15	85	
8	59158506:59558565	<i>UBXN2B</i>	LDL	13	87	[42]
			TC	15	85	
9	2454062:2854121	<i>VLDLR</i>	LDL	1	91	[43]
10	17079389:17479448	<i>VIM</i>	TC	5	93	[44]
10	94637063:95037122	<i>CYP26A1</i>	TG	3	95	[45]
12	111508189:111908248	<i>CUX2</i>	HDL	2	89	
			LDL	2	98	
			TC	2	98	
15	96517293:96917352	ENSG00000259359	HDL	2	87	
16	56310220:56710279	<i>OGFOD1</i>	TC	7	84	[46]
16	71894416:72310900	<i>HP</i>	LDL	1	97	[47]
			TC	1	97	
			TG	2	75	
		<i>HPR</i>	LDL	1	99	[48]
			TC	1	99	
			TG	2	89	
22	46433083:46833138	<i>PPARA</i>	TC	10	81	[49]

Signals not reported by Teslovich et al. with PP4 > 75% for colocalisation between the liver eQTL dataset and the Teslovich meta-analysis of LDL, HDL, TG, TC, using the strict prior $p_{12} = 10^{-6}$. For 11 genes with strong candidate status for lipid metabolism, we list a key reference that describes their function.

References

1. Teslovich TM, Musunuru K, Smith AV, Edmondson AC, Stylianou IM, et al. (2010) Biological, clinical and population relevance of 95 loci for blood lipids. *Nature* 466: 707–713.
2. Feero WG, Guttmacher AE, Manolio TA (2010) Genomewide association studies and assessment of the risk of disease. *New England Journal of Medicine* 363: 166–176.
3. Nica AC, Dermitzakis ET (2008) Using gene expression to investigate the genetic basis of complex disorders. *Human molecular genetics* 17: R129–R134.
4. Pickrell JK, Marioni JC, Pai AA, Degner JF, Engelhardt BE, et al. (2010) Understanding mechanisms underlying human gene expression variation with rna sequencing. *Nature* 464: 768–772.
5. Nica AC, Montgomery SB, Dimas AS, Stranger BE, Beazley C, et al. (2010) Candidate causal regulatory effects by integration of expression qtls with complex trait genetic associations. *PLoS genetics* 6: e1000895.
6. Hunt KA, Zhernakova A, Turner G, Heap GA, Franke L, et al. (2008) Newly identified genetic risk variants for celiac disease related to the immune response. *Nature genetics* 40: 395–402.
7. He X, Fuller CK, Song Y, Meng Q, Zhang B, et al. (2013) Sherlock: Detecting gene-disease associations by matching patterns of expression qtl and gwas. *The American Journal of Human Genetics* 92: 667–680.
8. Ding J, Gudjonsson JE, Liang L, Stuart PE, Li Y, et al. (2010) Gene expression in skin and lymphoblastoid cells: Refined statistical method reveals extensive overlap in cis-eqtl signals. *The American Journal of Human Genetics* 87: 779–789.
9. Flutre T, Wen X, Pritchard J, Stephens M (2013) A statistical framework for joint eqtl analysis in multiple tissues. *PLoS Genet* 9: e1003486.
10. Cotsapas C, Voight BF, Rossin E, Lage K, Neale BM, et al. (2011) Pervasive sharing of genetic effects in autoimmune disease. *PLoS genetics* 7: e1002254.
11. Plagnol V, Smyth DJ, Todd JA, Clayton DG (2009) Statistical independence of the colocalized association signals for type 1 diabetes and rps26 gene expression on chromosome 12q13. *Biostatistics* 10: 327–334.
12. Wallace C, Rotival M, Cooper JD, Rice CM, Yang JH, et al. (2012) Statistical colocalization of monocyte gene expression and genetic risk variants for type 1 diabetes. *Human molecular genetics* 21: 2815–2824.
13. Wallace C (2013) Unbiased statistical testing of shared genetic control for potentially related traits. *Genetic Epidemiology* (In Press), arXiv:13015510 .
14. Schadt EE, Woo S, Hao K (2012) Bayesian method to predict individual snp genotypes from gene expression data. *Nature genetics* 44: 603–608.
15. Marchini J, Howie B (2010) Genotype imputation for genome-wide association studies. *Nature Reviews Genetics* 11: 499–511.
16. Howie B, Marchini J, Stephens M (2011) Genotype imputation with thousands of genomes. *G3: Genes, Genomes, Genetics* 1: 457–470.

17. Howie B, Fuchsberger C, Stephens M, Marchini J, Abecasis GR (2012) Fast and accurate genotype imputation in genome-wide association studies through pre-phasing. *Nature genetics* .
18. Wakefield J (2009) Bayes factors for genome-wide association studies: comparison with p-values. *Genetic Epidemiology* 33: 79–86.
19. Brown CD, Mangravite LM, Engelhardt BE (2012) Integrative modeling of eqtls and cis-regulatory elements suggest mechanisms underlying cell type specificity of eqtls. *arXiv preprint arXiv:12103294* .
20. Trynka G, Hunt KA, Bockett NA, Romanos J, Mistry V, et al. (2011) Dense genotyping identifies and localizes multiple common and rare variant association signals in celiac disease. *Nature genetics* 43: 1193–1201.
21. Yang J, Ferreira T, Morris AP, Medland SE, Madden PA, et al. (2012) Conditional and joint multiple-snp analysis of gwas summary statistics identifies additional variants influencing complex traits. *Nature genetics* 44: 369–375.
22. Consortium GLG, et al. (2013) Discovery and refinement of loci associated with lipid levels. *Nature genetics* .
23. Newton R, Wernisch L (2007) Rweb: A web application to create user friendly web interfaces for r scripts. *New Functions for Multivariate Analysis* : 32.
24. Trabzuni D, Ryten M, Walker R, Smith C, Imran S, et al. (2012) Quality control parameters on a large dataset of regionally dissected human control brains for whole genome expression studies. *Journal of Neurochemistry* 120: 473–473.
25. Ramasamy A, Trabzuni D, Gibbs JR, Dillman A, Hernandez DG, et al. (2013) Resolving the polymorphism-in-probe problem is critical for correct interpretation of expression qtl studies. *Nucleic Acids Research* .
26. Guan Y, Stephens M (2008) Practical issues in imputation-based association mapping. *PLoS Genet* 4: e1000279.
27. Khatun J (2012) An integrated encyclopedia of dna elements in the human genome. *Nature* .
28. Gerstein MB, Kundaje A, Hariharan M, Landt SG, Yan KK, et al. (2012) Architecture of the human regulatory network derived from encode data. *Nature* 489: 91–100.
29. Wen X, Stephens M (2011) Bayesian methods for genetic association analysis with heterogeneous subgroups: from meta-analyses to gene-environment interactions. *arXiv preprint arXiv:11111210* .
30. Stephens M, Balding DJ (2009) Bayesian statistical methods for genetic association studies. *Nature Reviews Genetics* 10: 681–690.
31. Burton PR, Clayton DG, Cardon LR, Craddock N, Deloukas P, et al. (2007) Genome-wide association study of 14,000 cases of seven common diseases and 3,000 shared controls. *Nature* 447: 661–678.
32. Nicolae DL, Gamazon E, Zhang W, Duan S, Dolan ME, et al. (2010) Trait-associated snps are more likely to be eqtls: annotation to enhance discovery from gwas. *PLoS genetics* 6: e1000888.
33. Knight J, Barnes MR, Breen G, Weale ME (2011) Using functional annotation for the empirical determination of bayes factors for genome-wide association study analysis. *PloS one* 6: e14808.

34. Johansson M, Roberts A, Chen D, Li Y, Delahaye-Sourdeix M, et al. (2012) Using prior information from the medical literature in gwas of oral cancer identifies novel susceptibility variant on chromosome 4-the adapt method. *PloS one* 7: e36888.
35. Richards A, Jones L, Moskvina V, Kirov G, Gejman P, et al. (2011) Schizophrenia susceptibility alleles are enriched for alleles that affect gene expression in adult human brain. *Molecular psychiatry* 17: 193–201.
36. Dimas AS, Deutsch S, Stranger BE, Montgomery SB, Borel C, et al. (2009) Common regulatory variation impacts gene expression in a cell type–dependent manner. *Science* 325: 1246–1250.
37. Hernandez DG, Nalls MA, Moore M, Chong S, Dillman A, et al. (2012) Integration of gwas snps and tissue specific expression profiling reveal discrete eqtls for human traits in blood and brain. *Neurobiology of disease* .
38. Team RDC (2013) R: A Language and Environment for Statistical Computing. R Foundation for Statistical Computing, Vienna, Austria. URL <http://www.R-project.org>.
39. Yilmaz Y, Eren F, Colak Y, Senates E, Celikel CA, et al. (2012) Hepatic expression and serum levels of syndecan 1 (cd138) in patients with nonalcoholic fatty liver disease. *Scandinavian journal of gastroenterology* 47: 1488–1493.
40. Garver WS, Krishnan K, Gallagos JR, Michikawa M, Francis GA, et al. (2002) Niemann-pick c1 protein regulates cholesterol transport to the trans-golgi network and plasma membrane caveolae. *Journal of lipid research* 43: 579–589.
41. Johnson MP, Brennecke SP, East CE, Göring HH, Kent Jr JW, et al. (2012) Genome-wide association scan identifies a risk locus for preeclampsia on 2q14, near the inhibin, beta b gene. *PloS one* 7: e33666.
42. Wang CW, Lee SC (2012) The ubiquitin-like (ubx)-domain-containing protein ubx2/ubxd8 regulates lipid droplet homeostasis. *Journal of Cell Science* 125: 2930–2939.
43. Nasarre L, Juan-Babot O, Gastelurrutia P, Lluçia-Valldeperas A, Badimon L, et al. (2012) Low density lipoprotein receptor–related protein 1 is upregulated in epicardial fat from type 2 diabetes mellitus patients and correlates with glucose and triglyceride plasma levels. *Acta diabetologica* : 1–8.
44. Sarria A, Panini S, Evans R (1992) A functional role for vimentin intermediate filaments in the metabolism of lipoprotein-derived cholesterol in human sw-13 cells. *Journal of Biological Chemistry* 267: 19455–19463.
45. Loudig O, Maclean G, Dore N, Luu L, Petkovich M (2005) Transcriptional co-operativity between distant retinoic acid response elements in regulation of cyp26a1 inducibility. *Biochem J* 392: 241–248.
46. Saito K, Adachi N, Koyama H, Matsushita M (2010) Ogfod1, a member of the 2-oxoglutarate and iron dependent dioxygenase family, functions in ischemic signaling. *FEBS letters* 584: 3340–3347.
47. Wassell J, et al. (1999) Haptoglobin: function and polymorphism. *Clinical laboratory* 46: 547–552.
48. Nielsen MJ, Petersen SV, Jacobsen C, Oxvig C, Rees D, et al. (2006) Haptoglobin-related protein is a high-affinity hemoglobin-binding plasma protein. *Blood* 108: 2846–2849.
49. Staels B, Maes M, Zambon A (2008) Fibrates and future ppar α agonists in the treatment of cardiovascular disease. *Nature Clinical Practice Cardiovascular Medicine* 5: 542–553.

Bayesian Test for Colocalisation Between Pairs of Genetic Association Studies Using Summary Statistics

Claudia Giambartolomei^{1,*}, Damjan Vukcevic², Eric E. Schadt³, Lude Franke⁴, Aroon D. Hingorani⁵, Chris Wallace⁶, Vincent Plagnol¹

1 UCL Genetics Institute, University College London (UCL), Darwin Building, Gower Street, London WC1E 6BT, UK

2 Murdoch Childrens Research Institute, Royal Children's Hospital, Melbourne, Australia

3 Department of Genetics and Genomics Sciences, Mount Sinai School of Medicine, New York, New York, United States of America

4 Department of Genetics, University Medical Center Groningen, University of Groningen, Groningen, The Netherlands

5 Institute of Cardiovascular Science, University College London, London WC1E 6BT, UK

6 JDRF/Wellcome Trust Diabetes and Inflammation Laboratory, Cambridge, Institute for Medical Research, Department of Medical Genetics, NIHR, Cambridge Biomedical Research Centre, University of Cambridge, Addenbrooke's Hospital, Hills Rd, Cambridge, CB2 0XY, UK

* E-mail: claudia.giambartolomei.10@ucl.ac.uk

Supplementary material

Simplified model under assumption that all SNPs have the same prior

The probability space for a single SNP can be fully partitioned into (p_0, p_1, p_2, p_{12}) , where p_0 is the prior probability that a SNP is not associated with either trait, p_1 is defined as the prior probability that the SNP is only associated with trait 1, p_2 the prior probability that the SNP is associated only with trait 2, while p_{12} is the prior probability that the SNP is associated with both traits. We therefore have:

$$p_0 + p_1 + p_2 + p_{12} = 1$$

The priors p_0, p_1, p_2, p_{12} can vary across SNPs, for example depending on MAF, a measure of imputation quality, proximity to the promoter, function of the SNP. If however the priors do not vary across SNPs, then equation 1 in the main text becomes:

$$L(H_h) = L(H_h | D) = \sum_{S \in S_h} P(D | S)P(S) = P(S | S \in S_h) \times \sum_{S \in S_h} P(D | S) \quad (1)$$

This simplification is possible because each binary vector that belongs to the same set S_h has the same prior probability.

The prior probability of any one configuration in the different sets is:

- If $S \in S_0$, then $P(S) = p_0^Q$
- If $S \in S_1$, then $P(S) = p_0^{Q-1} \times p_1$
- If $S \in S_2$, then $P(S) = p_0^{Q-1} \times p_2$
- If $S \in S_3$, then $P(S) = p_0^{Q-2} \times p_1 \times p_2$
- If $S \in S_4$, then $P(S) = p_0^{Q-1} \times p_{12}$

Because we condition our analysis on having at most one association per trait, these probabilities should be normalised: $P(S) = p_0^Q / C$, where C is the sum of the probabilities associated with all the assignments that contain at most one association per trait. However, because subsequent derivations only consider the ratio of probabilities, the C term cancels out and this normalisation becomes unnecessary. Dividing each of these probabilities by $P(S_0)$ to obtain the ratio of prior odds, and since $p_0 \approx 1$, the second terms in equation 4 in the main text becomes:

- If $S \in S_0$, then $\frac{P(S)}{P(S_0)} = \frac{p_0^Q}{p_0^Q} = 1$
- If $S \in S_1$, then $\frac{P(S)}{P(S_0)} = \frac{p_0^{Q-1}}{p_0^Q} \times p_1 = \frac{p_1}{p_0} \approx p_1$
- If $S \in S_2$, then $\frac{P(S)}{P(S_0)} = \frac{p_0^{Q-1}}{p_0^Q} \times p_2 = \frac{p_2}{p_0} \approx p_2$
- If $S \in S_3$, then $\frac{P(S)}{P(S_0)} = \frac{p_0^{Q-2}}{p_0^Q} \times p_1 \times p_2 = \frac{p_1}{p_0} \times \frac{p_2}{p_0} \approx p_1 \times p_2$
- If $S \in S_4$, then $\frac{P(S)}{P(S_0)} = \frac{p_0^{Q-1}}{p_0^Q} \times p_{12} = \frac{p_{12}}{p_0} \approx p_{12}$

To compute the first terms in equation 4 in the main text, the BFs for each configuration in a set, we make use of the ABF derived for each SNP-trait association (section below). Two key assumptions are necessary for the following computations. Firstly that the traits are measured in unrelated individuals, and secondly that the effect sizes for the two traits are independent.

Putting the two terms together, we have:

- $L(H_0)/L(H_0) = 1$
- $L(H_1)/L(H_0) = p_1 \times \sum_{j=1}^Q ABF_j^1$
- $L(H_2)/L(H_0) = p_2 \times \sum_{j=1}^Q ABF_j^2$
- $L(H_3)/L(H_0) = p_1 \times p_2 \times \sum_{j,k,j \neq k} ABF_j^1 ABF_k^2$
- $L(H_4)/L(H_0) = p_{12} \times \sum_{j=1}^Q ABF_j^1 \times ABF_j^2$

Of note, we can also write:

$$L(H_3)/L(H_0) = p_1 \times p_2 \times \sum_{j=1}^Q ABF_j^1 \sum_{j=1}^Q ABF_j^2 - \left[\frac{p_1 \times p_2}{p_{12}} \times L(H_4)/L(H_0) \right]$$

Bayes factor computation

We assume that summary statistics for each SNP in the two datasets were obtained by fitting a generalised linear model with the phenotype as dependent variable and SNP genotype call as independent variable:

$$Y = \mu + \beta X$$

The Bayes factor quantities are estimated from summary statistics using the Asymptotic Bayes Factor derivation [1]. Using Wakefield's notations, under the null we assume that the effect size $\beta = 0$. Under the alternative, β is normally distributed with mean 0 and variance W .

To derive the ABF computation, Wakefield uses the fact that asymptotically $\hat{\beta} \rightarrow N(\beta, V)$. The distribution of the estimated regression parameters $\hat{\mu}$ and $\hat{\beta}$ is:

$$\begin{bmatrix} \hat{\mu} \\ \hat{\beta} \end{bmatrix} \sim N_{p+1} \left(\begin{bmatrix} \mu \\ \beta \end{bmatrix} \begin{bmatrix} \mathbb{I}_{\mu\mu} & \mathbb{I}_{\mu\beta} \\ \mathbb{I}_{\mu\beta}^T & \mathbb{I}_{\beta\beta} \end{bmatrix}^{-1} \right) \quad (2)$$

The intercept μ is a nuisance parameter which we can remove using the transformation:

$$\gamma = \mu + \frac{\mathbb{I}_{\mu\beta}}{\mathbb{I}_{\mu\mu}} \beta$$

In which case the previous equality becomes:

$$\begin{bmatrix} \hat{\gamma} \\ \hat{\beta} \end{bmatrix} \sim N_{p+1} \left(\begin{bmatrix} \gamma \\ \beta \end{bmatrix} \begin{bmatrix} \mathbb{I}_{\mu\mu}^* & 0 \\ 0^T & \mathbb{I}_{\beta\beta} \end{bmatrix}^{-1} \right) \quad (3)$$

This independence property can be combined with independent priors for both parameters so that one can only consider β and ignore the effect of the μ term. Hence, after applying the reparameterisation we have:

$$BF = \int \frac{f(\beta)}{f(0)} \pi(\beta) d\beta$$

Which then becomes (assuming normality and asymptotic behaviour):

$$ABF = \frac{1}{\sqrt{1-r}} \times \exp \left[-\frac{Z^2}{2} \times r \right]$$

where $Z = \hat{\beta}/\sqrt{V}$ is the Wald test statistic. The shrinkage factor r is the ratio of the variance of the prior and total variance ($r = W/(V + W)$). This ratio takes a value between 0 and 1 and measure the relative contributions of the prior (W) and likelihood (V) to the inference. Values of r closer to 1 indicate a larger contribution from the likelihood (i.e. the data). The asymptotic posterior distribution of β is $N(r\hat{\beta}, rV)$. As the sample size increases, $V \rightarrow 0$ and $r \rightarrow 1$, so that the posterior concentrates around the MLE. We can compute the Z statistic from the p -values of a standard regression output using $|z| = \Phi^{-1}(1 - p/2)$, where Φ^{-1} is the inverse normal cumulative. Otherwise we can compute the Wald statistics directly if the estimated regression coefficients $\hat{\beta}$ and their variances $var(\hat{\beta})$ are supplied.

Variance of the estimated effect size $Var(\hat{\beta}) = V$

The variance of the maximum likelihood estimate $\hat{\beta}$ (denoted by V) can be approximated using the allele frequency of the variant f , the sample size N and the case control ratio s for binary outcome. It is well established that the score statistic to test whether the effect size $\beta = 0$ is:

$$U = \sum_i (Y_i - \bar{Y}) X_j$$

Score test theory asserts that the variance of U under the null is the inverse of the variance of the estimated effect size $\hat{\beta}$, also under the null. $Var(U)$ under the null can be estimated in several ways, including the standard derivation of the Fisher information matrix [2].

We assume that the genotypes X are under Hardy Weinberg equilibrium. Hence X is drawn from a binomial distribution with success parameter f , which we use to denote the allele frequency.

$$Var[X_j] = 2f_j(1 - f_j)$$

where f_j is the population allele frequency of the SNP j .

When the dataset is a case-control (the trait Y is binomial):

$$Var[Y] = s(1 - s)$$

where s is the proportion of cases in the population. If the outcome variable Y is continuous we assume that Y is normalised such that $Var(Y) = 1$.

Putting together these equations, we have, in a case control setting:

$$V = Var(\hat{\beta}_j) = \frac{1}{Ns(1 - s) \times 2f_j(1 - f_j)}$$

Choice of priors for the probability that each variant affects the traits

The prior probabilities assigned to each SNP, p_0, p_1, p_2, p_{12} , are mutually exclusive events. The probability of a SNP being associated with both traits, p_{12} , can be interpreted using a conditional argument:

$$\begin{aligned} p_{12} &= \mathbb{P}(\text{SNP associated with both traits}) \\ &= \mathbb{P}(\text{SNP associated with trait 1}) \times \mathbb{P}(\text{SNP associated with trait 2} \mid \text{SNP associated with trait 1}) \end{aligned}$$

The conditional term in the right hand side of the equation above can be approximated as follows:

$$\begin{aligned} \mathbb{P}(\text{SNP associated with trait 2} \mid \text{SNP associated with trait 1}) &= \frac{p_{12}}{(p_{12} + p_1)} \\ &= \frac{10^{-6}}{(10^{-6} + 10^{-4})} \\ &\approx \frac{10^{-6}}{10^{-4}} \\ &\approx 0.01 \end{aligned}$$

So in terms of conditional probability, if we assume a prior probability of $p_{12} = 1 \times 10^{-6}$ and $p_1 = p_2 = 1 \times 10^{-4}$, then the prior assumption is that of all SNPs associated with trait 1, 1 in 100 of them will also be associated with trait 2. Since as we stated previously each SNP belongs to only one of the five sets corresponding to the five hypotheses, the probability of a SNP not being associated with either trait is: $p_0 = 1 - (p_1 + p_2 + p_{12}) \approx 0.9998 \approx 1$.

Choice of priors for the standard deviation W of the effect size parameter β

Prior standard deviation of the additive effect parameter β was set to 0.15 for a continuous trait. Owing to our assumption that $Var(Y) = 1$, this prior corresponds to a variance explained of ~ 0.01 for a variance with MAF of 30%.

In a case-control study, we set $W = 0.2$ for the variance of the log-odds ratio parameter, as was previously used in WTCCC [3], which corresponds to an inter-quartile range between 0.74 and 1.35 for the odds ratio parameter. The priors chosen for case-control and for quantitative traits are also very similar to the SNPTEST default ([4,5]).

Simulation procedure

To simulate the posterior probability of a common signal (“PP4”) under different scenarios, we used the imputed genotypes from two different datasets: Whitehall II study (WHII), a longitudinal prospective cohort study genotyped using the gene-centric Illumina MetaboChip [6,7], and the expression dataset described herein. We randomly chose a causal SNP A among genotyped and well imputed SNPs ($R_{sq} > 0.8$) from any genomic region in common between the two datasets.

The additive genetic variance explained by the locus is

$$Var[\beta X_A] = \beta_A^2 \times 2f_A(1 - f_A)$$

where f_A is the population allele frequency of the causal SNP A, and β_A is the additive effect (in standard deviations) [8].

For different variance explained for the causal SNP, depending on the simulation scenario, we computed the true effect at the causal SNP:

$$\beta_A = \sqrt{\frac{Var[\beta X_A]}{2f_A(1 - f_A)}}$$

We then simulated the phenotype of the i^{th} individual in each of the two datasets using the computed true effect β_A :

$$Y_i = x_{iA} \times \beta_A + e_i \quad \text{with } e_i \sim N(0,1)$$

where x_{iA} is the additive genetic value at the causal SNP of individual i and e_i is a random error drawn from a normal distribution with mean 0 and variance of 1.0.

To simulate p -values from different sample sizes using the original datasets, we computed the expected value of each estimated beta multiplying the pairwise correlation coefficient r between the causal SNP A and all other SNPs, by the true value of beta at the causal SNP:

The derivation of this equation is described in the following section.

The expected regression coefficient at a second SNP B in relation to the causal SNP A is then:

$$\beta_j = \beta_A r \sqrt{\frac{f_A(1 - f_A)}{f_j(1 - f_j)}}. \quad (4)$$

where f_j is a vector of β s for all SNPs excluding the causal SNP.

The difference between the regression coefficients $\hat{\beta}$ estimated from the glm and the expected value β , computed at each SNP, can be considered the standard error of the mean and it varies with $\frac{1}{\sqrt{(N)}}$, where N is the original sample size. When N is increased, the estimate becomes closer to the true value β , decreasing the variability of the estimator. Then the simulations with a larger sample size involves simply rescaling this difference:

$$(\hat{\beta} - \beta) \sqrt{\frac{N}{N.new}} \quad (5)$$

Then we can compute the new p -values from the new simulated estimates and standard deviations. We used this method to perform simulations to find sample size required for colocalisation analysis, and to find the consequence of using limited variant density.

Relationship between model parameters and LD

Equation 4 was first derived in [9], where the additive effects for case-control studies were shown to decay linearly, in proportion to r , the correlation between the causal and marker loci. Here we show the same relationship holds for quantitative traits.

We use the same LD model, and associated notation, as defined in [9]. To summarise briefly, let A and B be a pair of biallelic SNPs, with the alleles at each coded by 0 and 1. Let f_A be the population frequency of allele 1 at SNP A , and define f_B similarly for SNP B . Let r be the population correlation coefficient between them, the square of which is a commonly used measure of LD. We can define the following conditional probabilities on a haplotype level:

$$\begin{aligned} q_0 &= P(A = 1 \mid B = 0), \\ q_1 &= P(A = 1 \mid B = 1), \end{aligned}$$

These quantities were shown to be related by the identity,

$$r = (q_1 - q_0) \sqrt{\frac{f_B(1 - f_B)}{f_A(1 - f_A)}},$$

Let SNP A be a causal and SNP B be a marker. Define the following expectations:

$$\begin{aligned} a_0 &= \mathbb{E}(Y \mid A = 0), & b_0 &= \mathbb{E}(Y \mid B = 0), \\ a_1 &= \mathbb{E}(Y \mid A = 1), & b_1 &= \mathbb{E}(Y \mid B = 1), \\ a_2 &= \mathbb{E}(Y \mid A = 2), & b_2 &= \mathbb{E}(Y \mid B = 2). \end{aligned}$$

Relating these using the LD model gives,

$$\begin{aligned} b_0 &= a_0(1 - q_0)^2 + a_1 2q_0(1 - q_0) + a_2 q_0^2, \\ b_1 &= a_0(1 - q_0)(1 - q_1) + a_1(q_0(1 - q_1) + q_1(1 - q_0)) + a_2 q_0 q_1, \\ b_2 &= a_0(1 - q_1)^2 + a_1 2q_1(1 - q_1) + a_2 q_1^2. \end{aligned}$$

Combining and rearranging these gives,

$$b_1^2 - b_0 b_2 = (a_1^2 - a_0 a_2) (q_1 - q_0)^2.$$

If we consider an additive model, it is easy to show that $b_1^2 - b_0 b_2 = \beta_B^2$ and $a_1^2 - a_0 a_2 = \beta_A^2$. Putting these together gives,

$$\beta_B = \beta_A r \sqrt{\frac{f_A(1 - f_A)}{f_B(1 - f_B)}}. \quad (6)$$

Equation 6 is analogous to the respective results from [9] for binary traits. The main difference is that for quantitative traits here we have shown them to be exact. As before, we can see that the deviation effect decays more quickly with LD than does the additive effect: quadratically in r rather than linearly. This implies that the distortion effect described earlier for binary traits will extend also to quantitative traits.

Relationship between model parameters and LD using imputed genotypes

The previous section assumed the genotypes were observed without error. We can derive a similar relationship in the scenario where we instead use imputed genotype data.

Continuing with the same notation, we now allow A and B to have posterior distributions for each individual's genotype. The appropriate analysis should average the likelihood over these posteriors. A convenient approximation to this is to replace each genotype by its mean posterior value. [10] showed that this is a good approximation in the GWAS context. This leaves us in a similar situation as before, except that A and B have become continuous quantitative variables. The following general results apply for the regression parameters,

$$\beta_A = \frac{\text{cov}(Y, A)}{\text{var}(A)},$$

$$\beta_B = \frac{\text{cov}(Y, B)}{\text{var}(B)}.$$

We need two assumptions to complete the derivation. Firstly, we require that Y and B are conditionally independent given A . In other words, $\text{cov}(Y, B | A) = 0$. This is implicit in the definition of SNP A being the *causal* SNP, and is also implicitly assumed in the definitions in the previous section. The only extension here is that we assume this relationship still holds after imputation. This allows us to simplify the covariance of Y and B using the law of total covariance,

$$\begin{aligned} \text{cov}(Y, B) &= \mathbb{E}(\text{cov}(Y, B | A)) + \text{cov}(\mathbb{E}(Y | A), \mathbb{E}(B | A)) \\ &= \mathbb{E}(0) + \text{cov}(\mathbb{E}(Y | A), \mathbb{E}(B | A)) \\ &= \text{cov}(\mathbb{E}(Y | A), \mathbb{E}(B | A)). \end{aligned}$$

The second assumption we need is that the conditional expectations of Y and B on A are both linear in A . That is,

$$\begin{aligned} \mathbb{E}(Y | A) &= \theta_{Y0} + \theta_{Y1}A, \\ \mathbb{E}(B | A) &= \theta_{B0} + \theta_{B1}A. \end{aligned}$$

We already make this assumption for the relationship between Y and A , in using a linear regression model for the trait. The extra part here is that we assume the same type of relationship between the causal SNP and marker SNP. Since the underlying values for A and B are binary, this is reasonable.

Note that these are just standard linear regression equations, so we have that,

$$\begin{aligned} \theta_{Y1} &= \frac{\text{cov}(Y, A)}{\text{var}(A)}, \\ \theta_{B1} &= \frac{\text{cov}(B, A)}{\text{var}(A)}. \end{aligned}$$

Putting all of these formulae together gives,

$$\begin{aligned}
 \text{cov}(Y, B) &= \text{cov}(\mathbb{E}(Y | A), \mathbb{E}(B | A)) \\
 &= \text{cov}(\theta_{Y1}A, \theta_{B1}A) \\
 &= \theta_{Y1}\theta_{B1} \text{cov}(A, A) \\
 &= \frac{\text{cov}(Y, A) \text{cov}(B, A)}{\text{var}(A)}.
 \end{aligned}$$

Dividing both sides by $\text{var}(B)$ gives,

$$\begin{aligned}
 \frac{\text{cov}(Y, B)}{\text{var}(B)} &= \frac{\text{cov}(Y, A)}{\text{var}(A)} \frac{\text{cov}(B, A)}{\text{var}(B)} \\
 \frac{\text{cov}(Y, B)}{\text{var}(B)} &= \frac{\text{cov}(Y, A)}{\text{var}(A)} \frac{\text{cov}(B, A)}{\sqrt{\text{var}(A) \text{var}(B)}} \sqrt{\frac{\text{var}(A)}{\text{var}(B)}} \\
 \beta_B &= \beta_A \text{cor}(B, A) \sqrt{\frac{\text{var}(A)}{\text{var}(B)}} \\
 \beta_B &= \beta_A r \sqrt{\frac{\text{var}(A)}{\text{var}(B)}}.
 \end{aligned}$$

This formula is analogous to equation (6). Note that if A and B are observed without error then we recover the previous formula.

Simulations to find sample size required for colocalisation analysis

We used the simulation method described above to compare the distribution of $PP4$ of randomly sampled regions under different scenarios. We used the original sample size of the eQTL dataset ($n=966$) and a variance explained of 10% for expression, while varying the sample size of the biomarker dataset and the proportion of the biomarker's variance explained by the causal variant.

Simulations to find consequence of using limited variant density

We compared the $PP4$ of randomly sampled regions, using the simulation procedure described above, with the $PP4$ of the same regions after filtering for only the SNPs present in the Illumina 660K Chip (Figures S1 and S2). The original dataset based on > 990 genomes imputed data will be much denser than the Illumina dataset. This way we can consider the consequences of having imputed data versus genotyped data.

The same procedure is used to simulate the case when the causal SNP is not included in the data by excluding the causal SNP only from the Illumina dataset. All analyses were conducted in R [11].

Simulations for comparison with existing colocalisation tests

For simulations comparing proportional and Bayesian approaches, we sampled, with replacement, haplotypes of SNPs with a minor allele frequency of at least 5% found in phased > 990 Genomes Project data [12] across all 49 genomic regions outside the major histocompatibility complex (MHC) which have

been identified as type 1 diabetes (T1D) susceptibility loci to date, as summarised in T1DBase (Figures S3 and S4). [13]. These represent a range of region sizes and genomic topography typical of GWAS hits. We excluded the MHC region which is known to have high variation, strong LD and exhibits huge genetic influence on autoimmune disease risk involving multiple loci and hence requires individual treatment in any GWAS [14]. For each trait, we selected one or two “causal variants” at random, and simulated a Gaussian distributed quantitative trait for which each causal variant SNP explains a specified proportion of the variance. We either used all SNPs or the subset of SNPs which appear on the Illumina HumanOmniExpress genotyping array to conduct colocalisation testing to reflect the scenarios of very dense targeted genotyping *versus* a less dense GWAS chip. All analyses were conducted in R [11] using the `coloc` package for proportional colocalisation testing.

Supplementary Figures and Tables

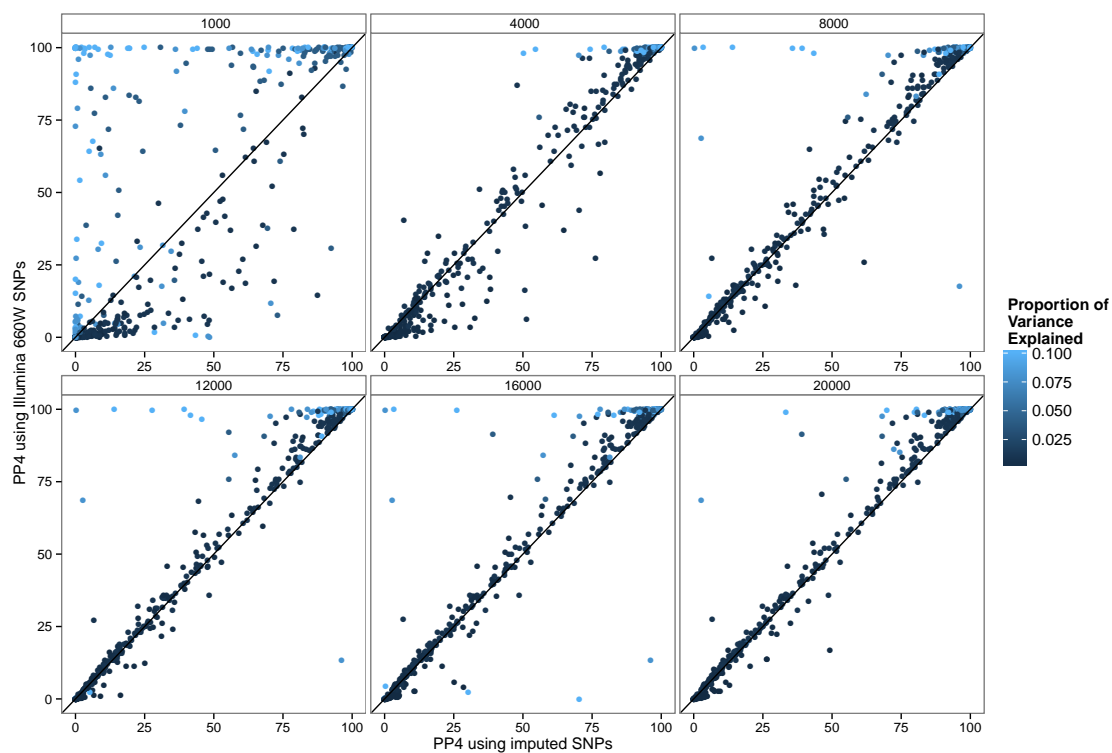


Figure S1. Simulation analysis with a shared causal variant between two studies, one eQTL (sample size 966 samples) and one biomarker, comparing results using imputed versus not imputed data where the causal SNP is included in both the cases. Each plot shows different sample sizes for one dataset. The variance explained by the causal variant for both the traits is colour coded. The x-axis shows the estimated PP4 for 1,000 simulations using data imputed from metaboChip Illumina array (Methods). The y-axis uses the same dataset restricted to variants present on the Illumina 660W genotyping array to assess the impact of a lower variant density. The causal variant is included in the Illumina 660W panel.

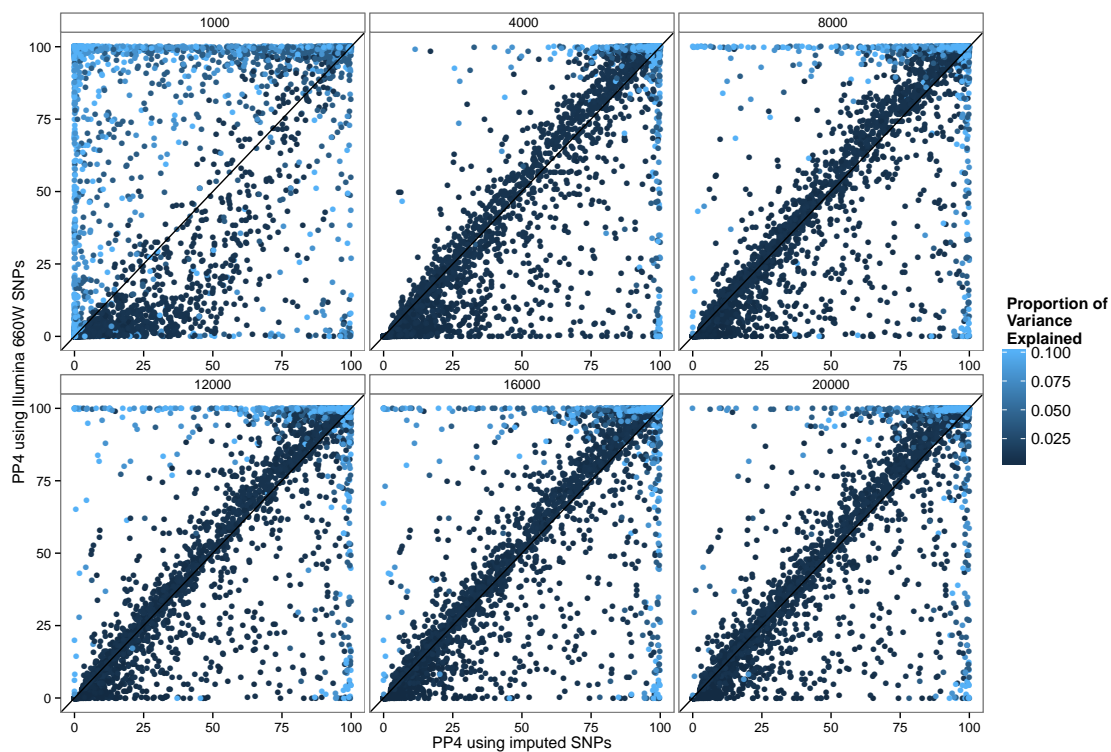


Figure S2. Simulation analysis with a shared causal variant between two studies, one eQTL (sample size 966 samples) and one biomarker, comparing results using imputed versus not imputed data where the causal SNP is not included in one of the datasets. Each plot shows different sample sizes for one dataset. The variance explained by the causal variant for both the traits is colour coded. Column and row headings are the same as in previous figure. The causal SNP is not included in Illumina 660W panel.

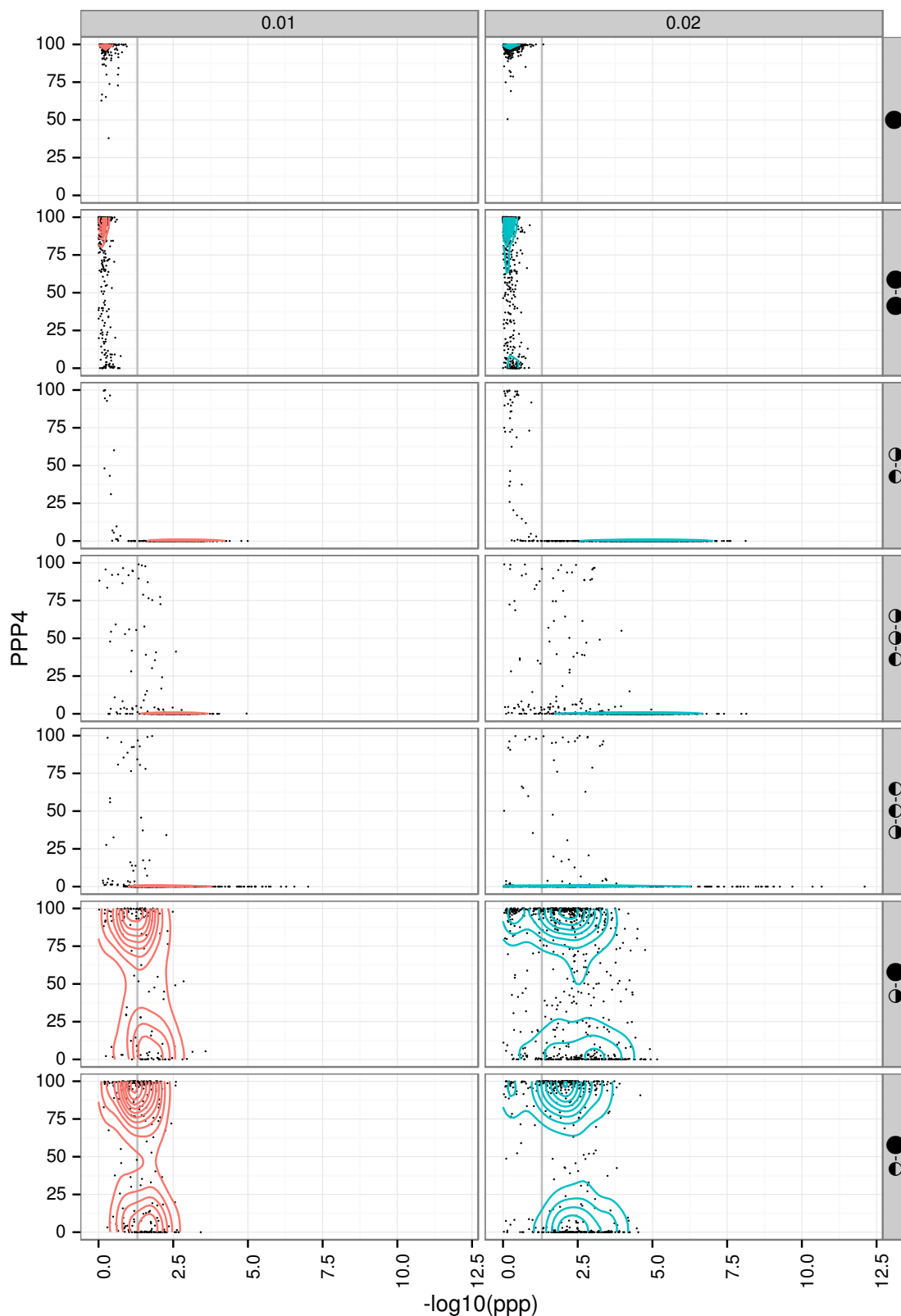


Figure S3. The relationship between PP4 and the posterior predictive p -value (on a $-\log_{10}$ scale) from proportional testing. Proportional testing uses the BMA approach, integrating over all possible two SNP models. Each row shows a different scenario, the total number of causal variants in a region is indicated by number of symbols in the plot titles with the type of causal variant indicated by the symbol: full circle - affects both traits; top only - affects one trait; bottom only- affects other trait. For proportional testing, the grey vertical line indicates the threshold ppp of 0.05. Each column shows the total proportion of trait variance for the biomarker explained by all variants in a region, with variance explained spread equally over all variants. In all cases, for the eQTL trait, $n=1,000$, 10% of the variance explained by the variant; for the biomarker trait, $n=10,000$.

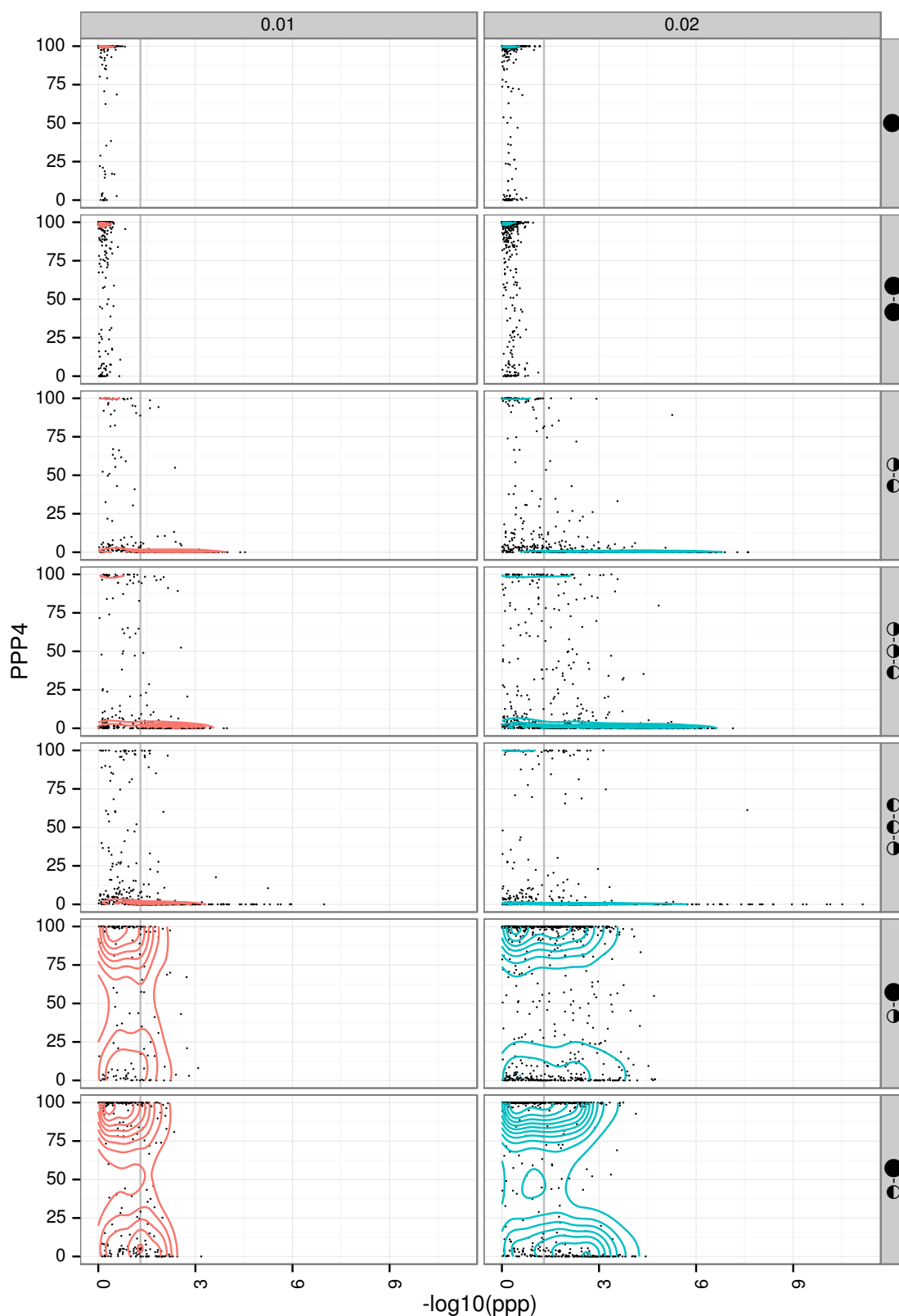
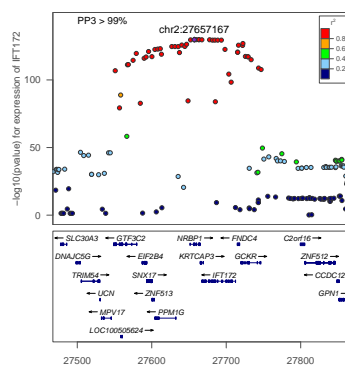
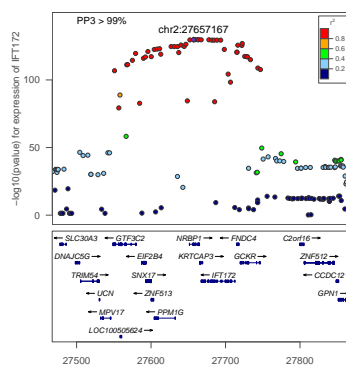
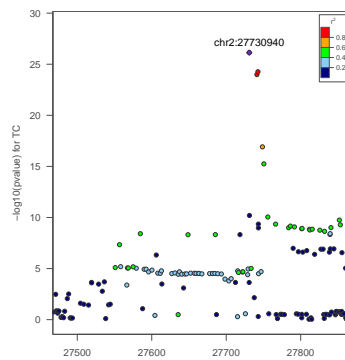
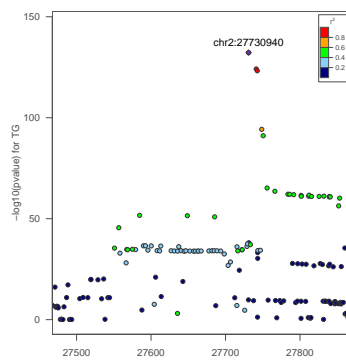
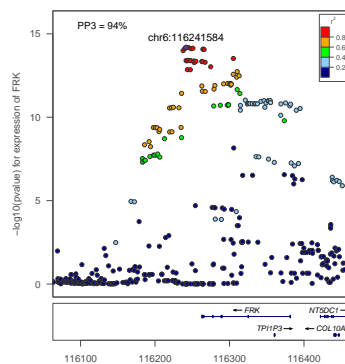
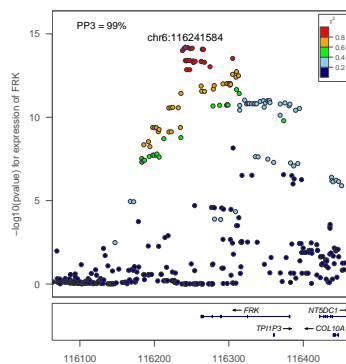
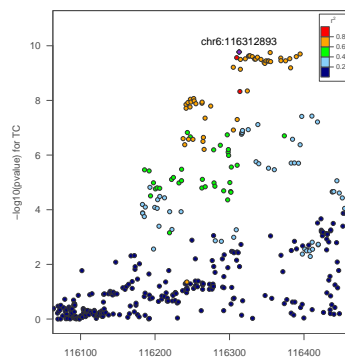
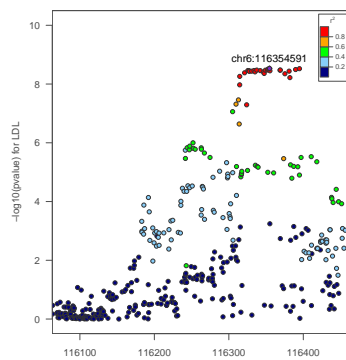


Figure S4. The relationship between PP4 and the posterior predictive p -value (on a $-\log_{10}$ scale) from proportional testing, using subset of SNPs which appear on the Illumina HumanOmniExpress genotyping array. For the eQTL trait, $n=1,000$, 10% of the variance explained by the variant; for the biomarker trait, $n=10,000$, 1% or 2% of the variance explained by the variant. Column and row headings are the same as in previous figure.



(1) IFT172/TG

(2) IFT172/TC



(3) FRK/LDL

(4) FRK/TC

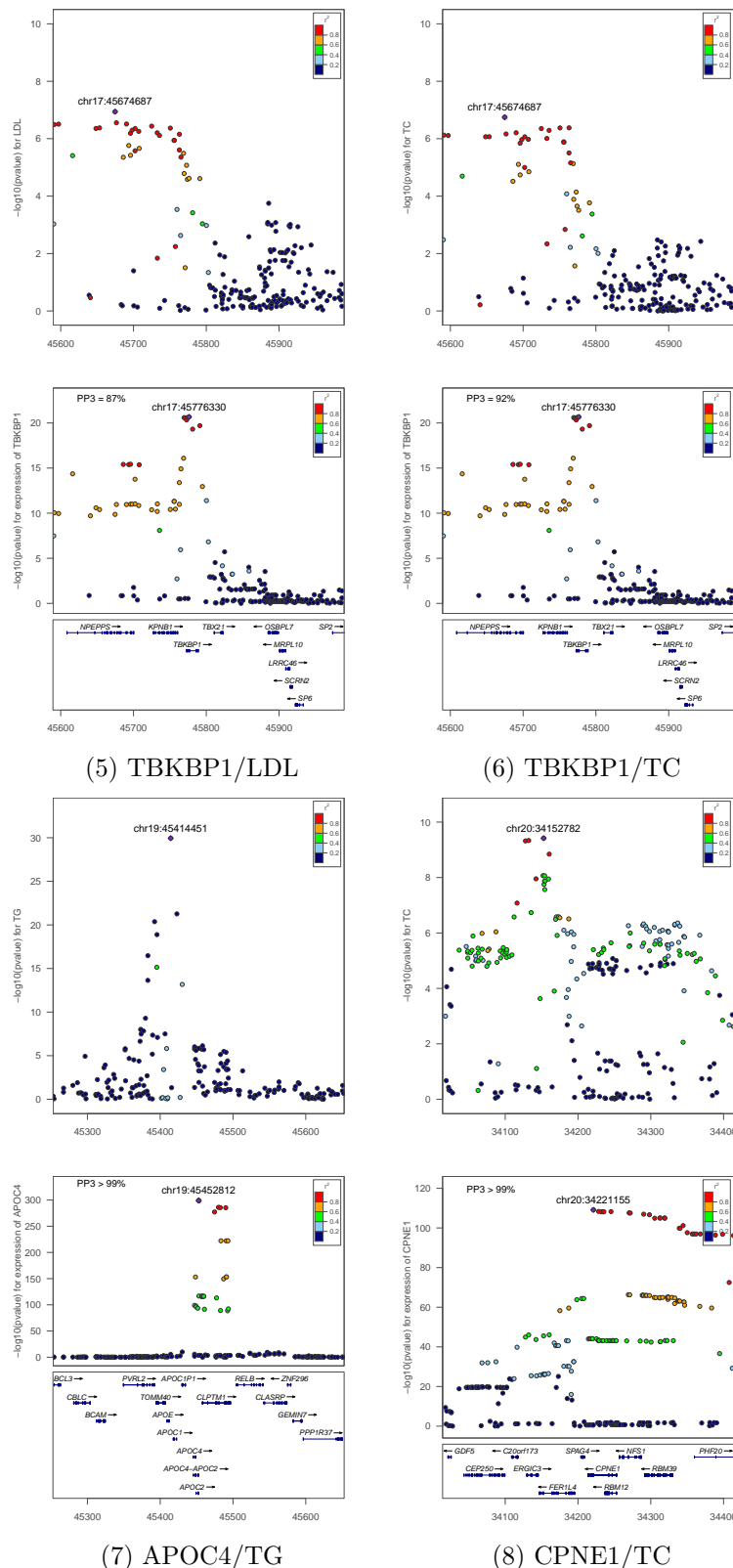


Figure S5. Regional Manhattan plots with $-\log_{10} p$ -value for loci reported in Teslovich et al. [15] as having a probable shared variant but not supported by our method based on PP4 (posterior probability for a shared signal values) $< 75\%$. The plots focus on a specific region of the genome with a range of ~ 400 kilobases around the expression probe of the gene specified below each plot. The top plots use the $-\log_{10}(p\text{-value})$ from the published meta-analysis with one of the four lipid biomarkers; the bottom plots show the $-\log_{10}(p\text{-value})$ computed by fitting a generalized linear model with expression as dependent variable and SNP genotypes as independent variable. Each dot represents one SNP, imputed or directly typed. The value on the top of each plot shows the PP4 from the colocalisation test between the two top SNP of the expression and biomarker associations.

Table S1. Results using reported loci that colocalise with liver eQTL

geneTranscriptsymbol	TranscriptPvalueTest	Trait	Chr	Region	Biom pval	Biom SNP	eQTL pval	eQTL SNP	Best Causal	$P_{12} = 10^{-5}$		$P_{12} = 2 \times 10^{-6}$		$P_{12} = 10^{-6}$		
										PP3 (%)	PP4 (%)	PP3 (%)	PP4 (%)	PP3 (%)	PP4 (%)	
RHCE	7.00E-54	LDL,TC	NA	NA	NA	NA	NA	NA	NA	NA	NA	NA	NA	NA	NA	NA
RHD	4.00E-08	LDL	1	25428038:25828097	1.20E-10	rs12027135	7.70E-11	rs909832	rs12027135	9	91	33	67	50	50	
			1	25456834:25856893	1.20E-10	rs12027135	0.0087	rs909832	rs12027135	< 1	2	< 1	< 1	< 1	< 1	
			1	25428038:25828097	4.10E-11	rs12027135	7.70E-11	rs909832	rs12027135	9	91	33	67	50	50	
			1	25456834:25856893	4.10E-11	rs12027135	0.0087	rs909832	rs12027135	< 1	2	< 1	< 1	< 1	< 1	
TMEM50A	4.00E-08	LDL	1	25488669:25888728	1.20E-10	rs12027135	4.40E-11	rs9689	rs10931242	12	88	41	59	58	42	
			1	25488669:25888728	4.10E-11	rs12027135	4.40E-11	rs9689	rs10931242	13	87	43	57	60	39	
TMEM57	2.00E-145	LDL	1	25626305:26026364	1.20E-10	rs12027135	2.10E-31	rs873308	rs12027135	1	99	5	94	10	90	
			1	25624780:26024839	1.20E-10	rs12027135	6.40E-08	rs686631	rs10903129	2	98	9	90	17	82	
			1	25625807:26025866	1.20E-10	rs12027135	7.60E-23	rs873308	rs873308	2	97	11	88	21	79	
			1	25626305:26026364	4.10E-11	rs12027135	2.10E-31	rs873308	rs12027135	1	99	5	94	11	89	
			1	25624780:26024839	4.10E-11	rs12027135	6.40E-08	rs686631	rs12027135	2	98	9	90	17	82	
ANGPTL3	1.00E-13	LDL	1	62870388:63270447	2.60E-18	rs3850634	1.90E-15	rs636497	rs3850634	9	91	15	85	26	74	
			1	62870388:63270447	4.90E-41	rs3850634	1.90E-15	rs636497	rs3850634	9	90	24	65	51	49	
			1	62870388:63270447	8.80E-43	rs2131925	1.90E-15	rs636497	rs2131925	8	92	29	70	45	54	
DOCK7	1.00E-22	LDL	1	62849818:63249877	2.60E-18	rs3850634	1.90E-25	rs11485618	rs3850634	5	95	23	77	37	63	
			1	62720869:63120928	2.60E-18	rs3850634	0.0049	rs10485659	rs3850634	1	13	2	3	2	1	
			1	62849818:63249877	4.90E-41	rs3850634	1.90E-25	rs11485618	rs10789118	5	95	20	80	33	67	
			1	62720869:63120928	4.90E-41	rs3850634	0.0049	rs10485659	rs3850634	1	14	2	3	2	1	
			1	62849818:63249877	8.80E-43	rs2131925	1.90E-25	rs11485618	rs2131925	5	94	23	77	37	63	
			1	62720869:63120928	8.80E-43	rs2131925	0.0049	rs10485659	rs2131925	1	14	2	3	2	1	
CELSR2	5.00E-94	LDL	1	109618271:110018330	9.70E-171	rs629301	1.50E-120	rs646776	rs629301	< 1	> 99	1	99	2	98	
			1	109618271:110018330	5.80E-131	rs629301	1.50E-120	rs646776	rs629301	< 1	> 99	1	99	3	97	
PSMA5	9.00E-17	LDL	1	109744528:110144587	9.70E-171	rs629301	1.50E-17	rs598939	rs629301	< 1	99	4	96	7	93	
			1	109741904:110141963	9.70E-171	rs629301	1.20E-07	rs600806	rs629301	98	1	99	< 1	99	< 1	
			1	109744528:110144587	5.80E-131	rs629301	1.50E-17	rs598939	rs629301	< 1	99	3	97	7	93	
PSRC1	2.00E-271	LDL	1	109741904:110141963	5.80E-131	rs629301	1.20E-07	rs600806	rs629301	98	1	99	< 1	99	< 1	
			1	109622208:110022267	9.70E-171	rs629301	1.10E-299	rs7528419	rs629301	< 1	99	3	97	7	93	
			1	109622208:110022267	5.80E-131	rs629301	1.10E-299	rs7528419	rs629301	< 1	99	3	96	7	93	
SORT1	2.00E-300	LDL	1	109652373:110052432	9.70E-171	rs629301	1.10E-299	rs7528419	rs629301	< 1	> 99	3	96	7	93	
			1	109656429:110056488	9.70E-171	rs629301	1.10E-299	rs7528419	rs629301	< 1	> 99	3	96	7	93	
			1	109652373:110052432	5.80E-131	rs629301	1.10E-299	rs7528419	rs629301	< 1	> 99	3	96	7	93	
SYPL2	1.00E-23	LDL	1	109824678:110224737	2.20E-64	rs672569	7.10E-103	rs1933182	rs1933182	> 99	< 1	> 99	< 1	> 99	< 1	
			1	109821999:110222054	2.90E-168	rs599839	0.0031	rs7536292	rs599839	< 1	> 99	< 1	< 1	< 1	< 1	
			1	109824678:110224737	8.00E-52	rs672569	7.10E-103	rs1933182	rs1933182	> 99	< 1	> 99	< 1	> 99	< 1	
			1	109821999:110222054	4.10E-130	rs599839	0.0031	rs7536292	rs599839	< 1	> 99	< 1	< 1	< 1	< 1	
IFT172	7.00E-32	TC	2	27467244:27867303	7.30E-27	rs1260326	1.70E-130	rs704791	rs704791	> 99	< 1	> 99	< 1	> 99	< 1	
			2	27467244:27867303	5.70E-133	rs1260326	1.70E-130	rs704791	rs1260326	> 99	< 1	> 99	< 1	> 99	< 1	
SLC39A8	3.00E-19	HDL	4	102982958:103383017	7.20E-11	rs13107325	3.80E-21	rs13107325	rs13107325	< 1	> 99	< 1	> 99	< 1	> 99	
			4	102972446:103372505	7.20E-11	rs13107325	0.027	rs11733483	rs13107325	< 1	> 99	< 1	> 99	< 1	> 99	
HLA-DQB1	2.00E-13	TC	6	32427977:32828028	2.60E-17	rs17533167	2.10E-43	rs13129720	rs13129720	> 99	< 1	> 99	< 1	> 99	< 1	
HLA-DRB1	7.00E-44	TC	6	32346553:32746610	4.00E-19	rs3177928	1.90E-217	rs477515	rs477515	> 99	< 1	> 99	< 1	> 99	< 1	
FRK	4.00E-12	LDL	6	116062804:116462863	2.90E-09	rs11153594	6.60E-15	rs195517	rs195517	90	10	98	2	99	1	
			6	116062804:116462863	1.70E-10	rs9488822	6.60E-15	rs195517	rs9488822	61	39	89	11	94	6	
PPP1R3B	1.00E-14	LDL	8	8793929:9193988	7.40E-15	rs2126259	1.90E-17	rs2126259	rs2126259	< 1	> 99	2	98	4	96	
			8	8795514:9195573	9.00E-24	rs2126259	6.20E-17	rs2126259	rs2126259	< 1	> 99	2	98	3	95	
			8	8793929:9193988	9.00E-24	rs2126259	1.90E-17	rs2126259	rs2126259	1	98	4	92	14	87	
			8	8793929:9193988	6.40E-25	rs9987289	6.20E-17	rs2126259	rs9987289	< 1	> 99	2	98	4	96	
			8	8795514:9195573	6.40E-25	rs9987289	1.90E-17	rs4240624	rs9987289	1	98	7	93	14	86	
TTC39B	2.00E-15	HDL	9	14971602:15371661	1.30E-13	rs643531	8.10E-18	rs581080	rs686030	2	98	10	89	19	81	
SPTY2D1	1.00E-16	TC	11	18429356:18829415	2.50E-08	rs10832963	7.20E-17	rs10832963	rs10832963	< 1	99	3	97	6	94	
			11	18427988:18828047	2.50E-08	rs10832963	2.90E-19	rs10832963	rs10832963	< 1	99	3	97	6	94	
FADS1	5.00E-18	LDL	11	61367291:61767350	1.20E-21	rs174583	2.90E-20	rs102275	rs102275	2	98	9	91	17	83	
			11	61367291:61767350	2.10E-22	rs174550	2.90E-20	rs102275	rs102275	1	99	7	93	13	87	
			11	61367291:61767350	5.40E-24	rs174546	2.90E-20	rs102275	rs102275	1	99	5	95	10	90	
ST3GAL4	2.00E-22	HDL	11	61367291:61767350	1.50E-22	rs174601	2.90E-20	rs102275	rs102275	< 1	99	4	96	8	92	
			11	126084467:126484526	1.20E-15	rs11220462	7.20E-25	rs4307732	rs4307732	2	98	8	92	15	85	
			11	126084467:126484526	2.10E-11	rs11220463	7.20E-25	rs4307732	rs7951028	1	99	7	93	13	87	
MMAB	2.00E-44	HDL	12	109793364:110193423	6.90E-15	rs7134594	1.00E-38	rs7954144	rs7954144	2	97	12	88	21	79	
NYNRRIN	3.00E-46	LDL	14	24688259:25088318	4.40E-11	rs2332328	1.10E-78	rs6573778	rs6573778	< 1	99	3	97	5	95	
CKMT1A	8.00E-28	TG	15	43791310:44191369	4.70E-08	rs9989313	1.20E-13	rs2260160	rs9989313	5	95	10	79	33	66	
ALDH1A2	5.00E-08	TC	15	58334099:58734158	8.80E-20	rs1532085	5.00E-45	rs1532085	rs1532085	< 1	> 99	1	99	2	98	
			15	58045824:58445883	0.0042	rs4646590	0.0027	rs9796698	rs9796698	< 1	> 99	< 1	< 1	< 1	< 1	
			15	58334099:58734158	2.90E-96	rs1532085	5.00E-45	rs1532085	rs1532085	< 1	> 99	< 1	> 99	< 1	> 99	
			15	58045824:58445883	0.0014	rs6493966	0.0027	rs9796698	rs8042066	< 1	> 99	< 1	< 1	< 1	< 1	
			15	58334099:58734158	2.40E-13	rs261342	5.00E-									

ANGPTL4	4.00E-08	HDL	18	46918514:47318573	2.70E-49	rs7241918	1.20E-11	rs4939883	rs4939883	< 1	> 99	2	98	4	96
APOC4	4.00E-09	HDL	19	8239194:8639253	3.20E-08	rs7255436	3.80E-09	rs7255436	rs7255436	< 1	> 99	2	98	5	95
		TG	19	45248464:45648523	1.10E-30	rs439401	9.40E-15	rs439401	rs439401	98	2	> 99	< 1	> 99	< 1
			19	45252653:45652712	1.10E-30	rs439401	1.10E-299	rs1130742	rs1130742	> 99	< 1	> 99	< 1	> 99	< 1
LILRA3	9.00E-12	HDL	19	54602026:55002085	4.30E-16	rs386000	8.20E-17	rs386000	rs386000	< 1	> 99	4	95	9	91
CEP250	3.00E-08	TC	20	33899702:34299761	3.80E-10	rs2277862	0.022	rs17424259	rs2104417	< 1	< 1	< 1	< 1	< 1	< 1
CPNE1	7.00E-41	TC	20	34013995:34414054	3.80E-10	rs2277862	7.30E-110	rs6060524	rs6060524	95	5	99	1	99	< 1
PLTP	3.00E-18	TG	20	44327404:44727463	4.70E-18	rs4810479	1.80E-20	rs6065906	rs4810479	< 1	> 99	3	97	5	95
		HDL	20	44327404:44727463	1.90E-22	rs6065906	1.80E-20	rs6065906	rs6065906	< 1	> 99	2	98	5	95
UBE2L3	6.00E-13	HDL	22	21778264:22178323	1.10E-08	22:21932068	8.90E-13	rs4821112	rs2283790	3	96	16	84	27	72

Published results of loci correlating with both liver expression and one of the four lipid traits (Teslovich et al. Supplementary Table 8) and posterior probability of different signal (PP3) and common signal (PP4) after applying colocalisation test. Each row lists the results for one probe, and the multiple entries for the same locus and trait represent multiple probes mapping to the same locus. the columns **Biom pval** and **eQTL pval** report the lowest p-value found for the association with the trait listed and for the liver expression association respectively, with the corresponding SNP name (**Biom SNP** and **eQTL SNP**); the column **Best Causal** reports the SNP within the region with the highest posterior probability to be the true causal variant. The probabilities have been rounded to 1 significant figure.

Table S2. eQTL/LDL colocalisation

Chr	Region	Signal	PP.H3.abf	PP.H4.abf	Tesl	Biom pval	Biom SNP	eQTL pval	eQTL SNP	Best Causal
1	109618271:110144587	CELSR2	2	98	Y	9.70E-171	rs629301	1.50E-120	rs646776	rs629301
		PSRC1	7	93	Y	9.70E-171	rs629301	1.10E-299	rs7528419	rs629301
		SORT1	7	93	Y	9.70E-171	rs629301	1.10E-299	rs7528419	rs629301
		PSMA5	7	93	Y	9.70E-171	rs629301	1.50E-17	rs599839	rs629301
1	150767063:151167122	ANXA9	3	97	N	6.50E-08	rs267733	6.10E-08	rs267734	rs267733
1	25626305:26026364	TMEM57	10	90	Y	1.20E-10	rs12027135	2.10E-31	rs873308	rs12027135
2	120908798:121308857	INHBB	7	77	N	3.80E-07	rs2030746	4.90E-21	rs17050272	rs17050272
8	59158506:59558565	UBXN2B	13	87	N	3.90E-09	rs1030431	3.50E-10	rs11996829	rs13263105
8	8795514:9392282	PPP1R3B	4	96	Y	7.40E-15	rs2126259	6.20E-17	rs2126259	rs2126259
		ENSG00000254235	13	87	N	7.40E-15	rs2126259	4.00E-13	rs4841133	rs9987289
9	2454062:2854121	VLDLR	1	91	N	8.00E-06	rs3780181	1.40E-07	rs3780181	rs3780181
11	126084467:126484526	ST3GAL4	15	85	Y	1.20E-15	rs11220462	7.20E-25	rs4307732	rs4307732
11	18429356:18829415	SPTY2D1	6	93	N	2.90E-07	rs10128711	7.20E-17	rs10832963	rs10832963
11	61367291:61767350	FADS1	17	83	Y	1.20E-21	rs174583	2.90E-20	rs102275	rs102275
12	111508189:111908248	CUX2	2	98	N	1.50E-09	rs11065987	1.00E-17	rs4378452	rs3184504
14	24688259:25088318	NYNRIN	5	95	Y	4.40E-11	rs2332328	1.10E-78	rs6573778	rs6573778
16	71894416:72310900	HP	1	97	N	1.80E-22	rs2000999	1.30E-05	rs2000999	rs2000999
		HPR	1	99	N	1.80E-22	rs2000999	4.20E-08	rs2000999	rs2000999
17	45562645:45962704	KPNB1	16	83	N	1.10E-07	rs8072100	3.10E-09	rs4794048	rs8072100
20	12947054:13347113	SPTLC3	4	86	N	4.20E-06	rs364585	2.30E-41	rs168622	rs364585

Positive (PP4 > 75%) eQTL/LDL colocalisation results between the liver eQTL dataset and the Teslovich meta-analysis using the most stringent prior for the probability that one SNP is associated with both traits, $p_{12} = 10^{-6}$. The column **Signal** includes genes that are part of overlapping regions and that colocalise at PP4 > 75%; the column **Region** represents the genomic coordinates for the start and stop of the signal; in the column **Tesl**, “Y” indicates that this signal with any of the genes included has been reported to be an intermediate for any of the four lipid biomarker associations by Teslovich et al. ; the columns **Biom pval** and **eQTL pval** report the lowest p-value found for LDL association and for the expression association respectively, with the corresponding SNP name (**Biom SNP** and **eQTL SNP**); the column **Best Causal** reports the SNP within the region with the highest posterior probability to be the true causal variant. The probabilities have been rounded to 1 significant figure.

Table S3. eQTL/HDL colocalisation

Chr	Region	Signal	PP.H3.abf	PP.H4.abf	Tesl	Biom pval	Biom SNP	eQTL pval	eQTL SNP	Best Causal
1	109618271:110144587	CELSR2	3	97	N	6.20E-08	rs629301	1.50E-120	rs646776	rs646776
		PSRC1	7	93	N	6.20E-08	rs629301	1.10E-299	rs7528419	rs629301
		SORT1	7	93	N	6.20E-08	rs629301	1.10E-299	rs7528419	rs629301
		PSMA5	7	92	N	6.20E-08	rs629301	1.50E-17	rs599839	rs12740374
2	85349026:85749085	TGOLN2	17	83	N	1.00E-07	rs1053560	2.80E-80	rs1044973	rs1044973
4	102982958:103383017	SLC39A8	1	99	Y	7.20E-11	rs13107325	3.80E-21	rs13107325	rs13107325
8	8795514:9392282	PPP1R3B	14	86	Y	6.40E-25	rs9987289	1.90E-17	rs4240624	rs9987289
		ENSG00000254235	4	96	N	6.40E-25	rs9987289	4.00E-13	rs4841133	rs9987289
9	14971602:15371661	TTC39B	19	81	Y	1.30E-13	rs643531	8.10E-18	rs581080	rs686030
11	61367291:61767350	FADS1	8	92	Y	1.50E-22	rs174601	2.90E-20	rs102275	rs102275
12	109793364:110193423	MMAB	21	79	Y	6.90E-15	rs7134594	1.00E-38	rs7954144	rs7954144
12	111508189:111908248	CUX2	2	89	N	4.40E-06	rs4766578	2.80E-16	rs3184504	rs3184504
15	58334099:59053162	ALDH1A2	1	99	Y	2.90E-96	rs1532085	5.00E-45	rs1532085	rs1532085
		LIPC	3	97	Y	2.90E-96	rs1532085	1.10E-25	rs2043085	rs1532085
15	96517293:96917352	ENSG00000259359	2	87	N	8.00E-06	rs8023580	5.50E-13	rs8023580	rs8023580
18	46918514:47318573	LIPG	4	96	Y	2.70E-49	rs7241918	1.20E-11	rs4939883	rs4939883
19	54578320:55002085	LILRB2	9	88	N	4.30E-16	rs386000	1.70E-06	rs416867	rs386000
		LILRA3	9	91	Y	4.30E-16	rs386000	8.20E-17	19:54793830	rs386000
19	8239194:8639253	ANGPTL4	5	95	Y	3.20E-08	rs7255436	3.80E-09	rs7255436	rs7255436
20	44327404:44727463	PLTP	5	95	Y	1.90E-22	rs6065906	1.80E-20	rs6065906	rs6065906

Positive (PP4 > 75%) eQTL/HDL colocalisation results between the liver eQTL dataset and the Teslovich meta-analysis. Column and row headings are the same as in previous figure.

Table S4. eQTL/TG colocalisation

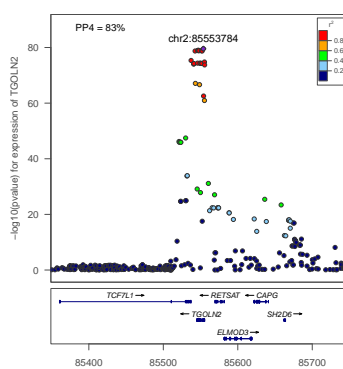
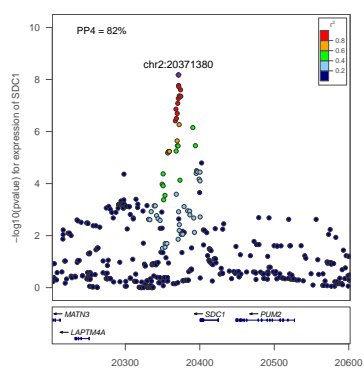
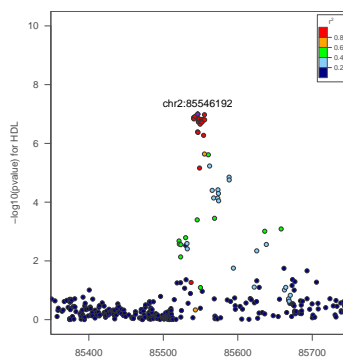
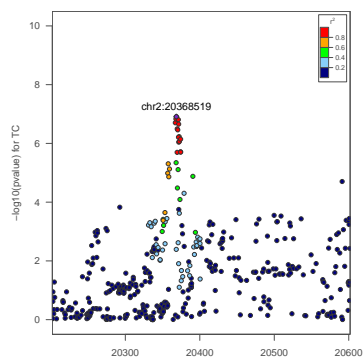
Chr	Region	Signal	PP.H3.abf	PP.H4.abf	Tesl	Biom pval	Biom SNP	eQTL pval	eQTL SNP	Best Causal
2	2754647:28005583	GCKR	5	77	N	5.70E-133	rs1260326	1.50E-05	rs1260326	rs1260326
		C2orf16	4	81	N	5.70E-133	rs1260326	8.30E-06	rs1260326	rs1260326
10	94637063:95037122	CYP26A1	3	95	N	2.40E-08	rs2068888	3.50E-06	rs4418728	rs2068888
11	61367291:61767350	FADS1	10	90	Y	5.40E-24	rs174546	2.90E-20	rs102275	rs102275
15	58653103:59053162	LIPC	19	81	Y	2.40E-13	rs261342	1.10E-25	rs2043085	rs2043085
16	30904631:31304682	VKORC1	23	77	Y	3.30E-08	rs11649653	1.10E-80	rs749671	rs749671
		ENSG00000255439	23	77	N	3.30E-08	rs11649653	1.10E-80	rs749671	rs749671
16	71894416:72310900	HP	2	75	N	5.70E-06	rs2000999	2.10E-06	rs2000999	rs2000999
		HPR	2	89	N	5.70E-06	rs2000999	4.20E-08	rs2000999	rs2000999
20	44327404:44727463	PLTP	5	95	Y	4.70E-18	rs4810479	1.80E-20	rs6065906	rs4810479

Positive (PP4 > 75%) eQTL/TG colocalisation results between the liver eQTL dataset and the Teslovich meta-analysis. Column and row headings are the same as in previous figure.

Table S5. eQTL/TC colocalisation

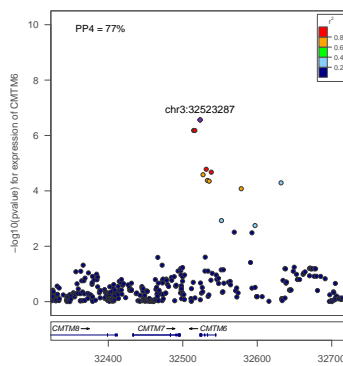
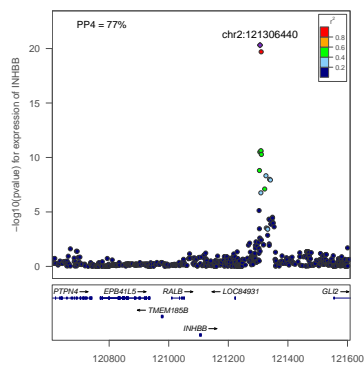
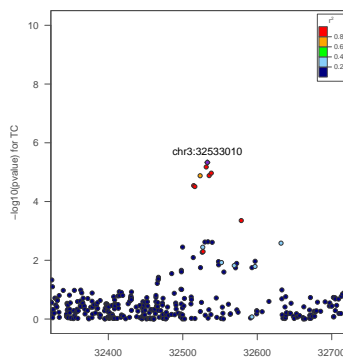
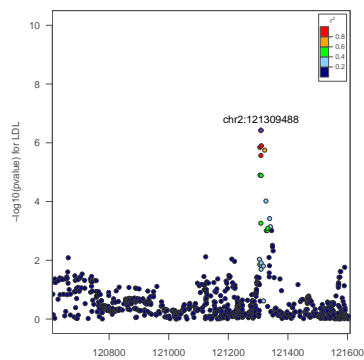
Chr	Region	Signal	PP.H3.abf	PP.H4.abf	Tesl	Biom pval	Biom SNP	eQTL pval	eQTL SNP	Best Causal
1	109618271:110144587	CELSR2	3	97	Y	5.80E-131	rs629301	1.50E-120	rs646776	rs629301
		PSRC1	7	93	Y	5.80E-131	rs629301	1.10E-299	rs7528419	rs629301
		SORT1	7	93	Y	5.80E-131	rs629301	1.10E-299	rs7528419	rs629301
		PSMA5	7	93	Y	5.80E-131	rs629301	1.50E-17	rs599839	rs629301
1	25626305:26026364	TMEM57	11	89	Y	4.10E-11	rs12027135	2.10E-31	rs873308	rs12027135
2	20201795:20601854	SDC1	17	82	N	1.20E-07	rs1473886	6.70E-09	rs907866	rs1107851
2	27546474:28005583	GCKR	5	77	N	7.30E-27	rs1260326	1.50E-05	rs1260326	rs1260326
		C2orf16	4	81	N	7.30E-27	rs1260326	8.30E-06	rs1260326	rs1260326
3	32322873:32722932	CMTM6	8	77	N	9.10E-07	rs7640978	2.70E-07	rs17029597	rs17029597
6	34355095:34755154	C6orf106	15	85	N	4.70E-11	rs2814982	4.50E-09	rs3800461	rs3800461
8	59158506:59558565	UBXN2B	15	85	N	8.80E-13	rs1030431	3.50E-10	rs11996829	rs13263105
8	8795514:9195573	PPP1R3B	3	97	Y	9.00E-24	rs2126259	6.20E-17	rs2126259	rs2126259
9	14971602:15371661	TTC39B	1	99	N	3.10E-09	rs581080	8.10E-18	rs581080	rs581080
10	17079389:17479448	VIM	5	93	N	7.20E-07	rs7903259	9.80E-09	rs10904908	rs7903259
11	126084467:126484526	ST3GAL4	13	87	Y	2.10E-11	rs11220463	7.20E-25	rs4307732	rs7951028
11	18429356:18829415	SPTY2D1	6	94	Y	2.50E-08	rs10832963	7.20E-17	rs10832963	rs10832963
11	61367291:61767350	FADS1	13	87	Y	2.10E-22	rs174550	2.90E-20	rs102275	rs102275
12	111508189:111908248	CUX2	2	98	N	2.40E-11	rs4766578	2.80E-16	rs3184504	rs3184504
14	24688259:25088318	NYNRIN	3	97	N	1.10E-07	rs6573778	1.10E-78	rs6573778	rs6573778
15	58334099:59053162	ALDH1A2	2	98	Y	8.80E-20	rs1532085	5.00E-45	rs1532085	rs1532085
		LIPC	3	97	Y	8.80E-20	rs1532085	1.10E-25	rs2043085	rs2043085
16	56310220:56710279	OGFOD1	7	84		3.20E-06	rs11644679	3.40E-11	rs11649379	rs11644679
16	71894416:72310900	HP	1	97	N	3.20E-24	rs2000999	2.10E-06	rs2000999	rs2000999
		HPR	1	99	N	3.20E-24	rs2000999	4.20E-08	rs2000999	rs2000999
17	45562645:45962704	KPNB1	13	86	N	1.80E-07	rs8072100	3.10E-09	rs4794048	rs8072100
18	46918514:47318573	LIPG	11	89	Y	2.00E-19	rs7239867	1.20E-11	rs4939883	rs4939883
22	46433083:46833138	PPARA	10	81	N	3.60E-06	rs4253772	6.00E-08	rs11704979	rs4253772

Positive (PP4 > 75%) eQTL/TC colocalisation results between the liver eQTL dataset and the Teslovich meta-analysis. TC column and row headings are the same as in previous figure.



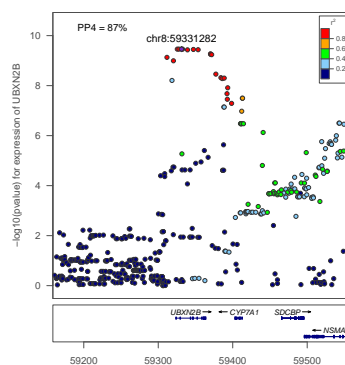
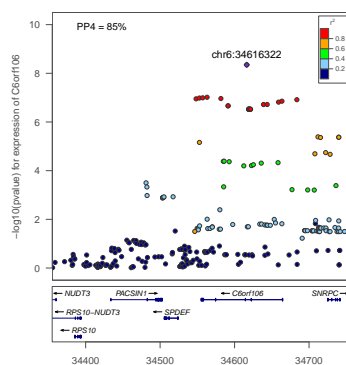
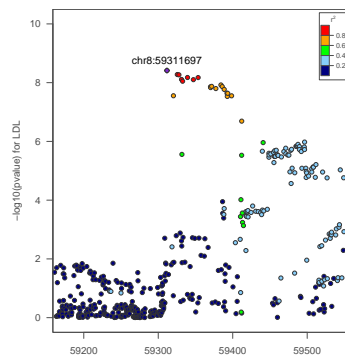
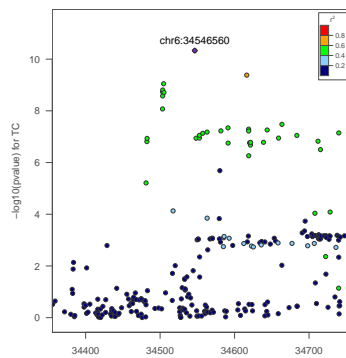
(1) SDC1/TC

(2) TGOLN2/HDL



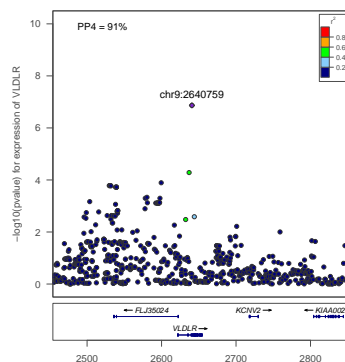
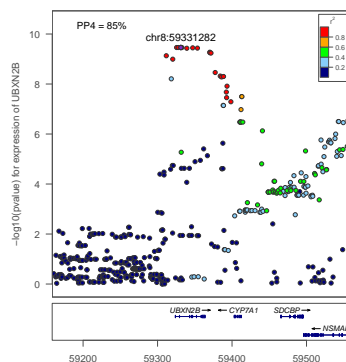
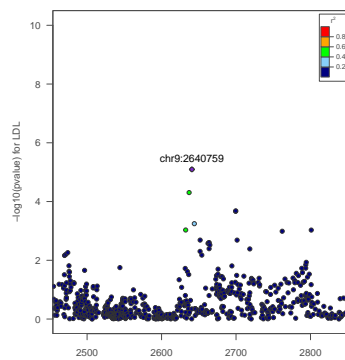
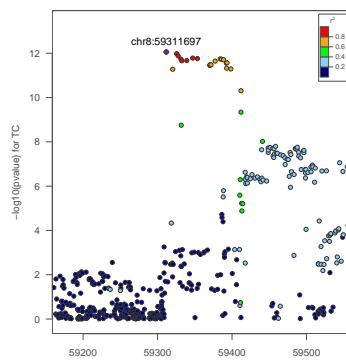
(3) INHBB/LDL

(4) CMTM6/TC



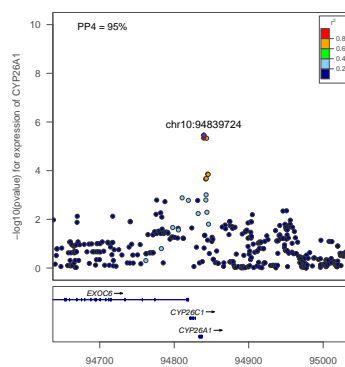
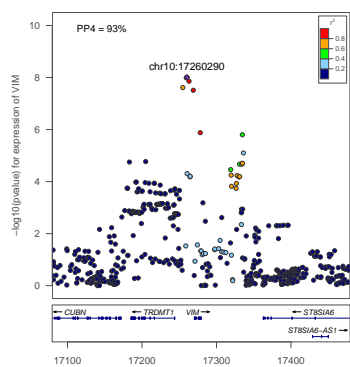
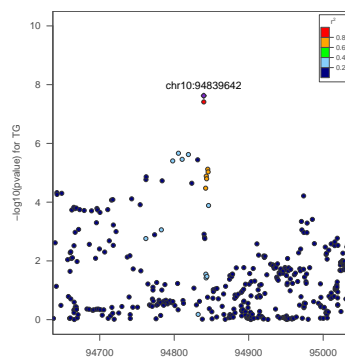
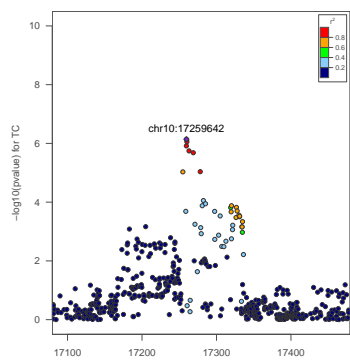
(5) C6orf106/TC

(6) UBXL2B/LDL



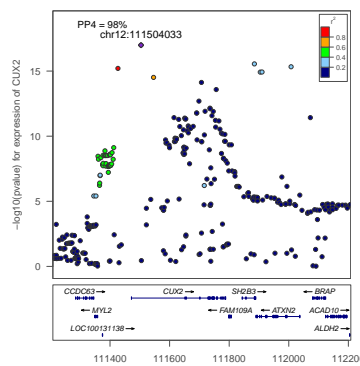
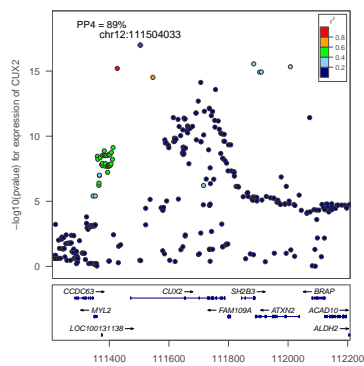
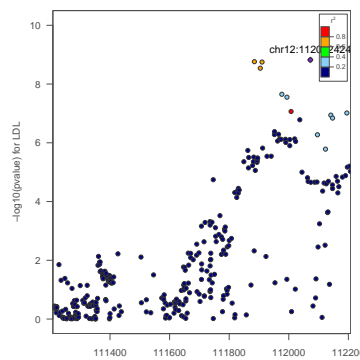
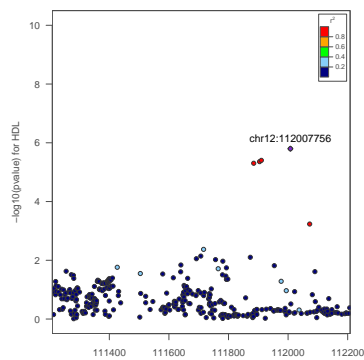
(7) UBXL2B/TC

(8) VLDL/LDL



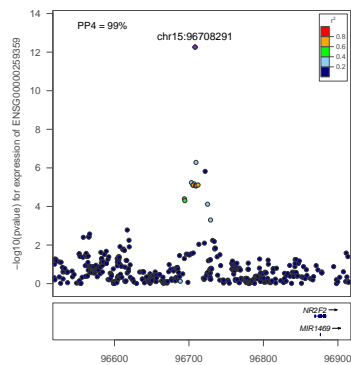
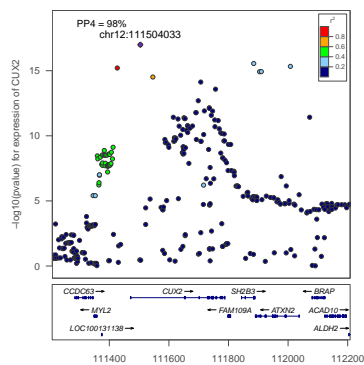
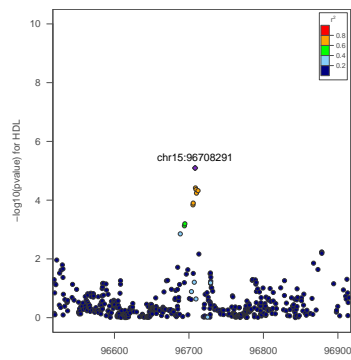
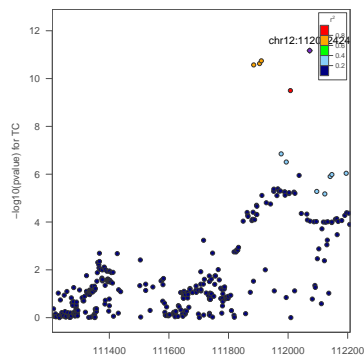
(9) VIM/TC

(10) CYP26A1/TG



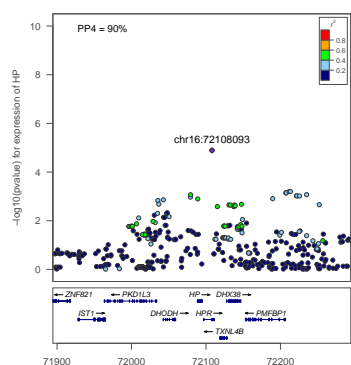
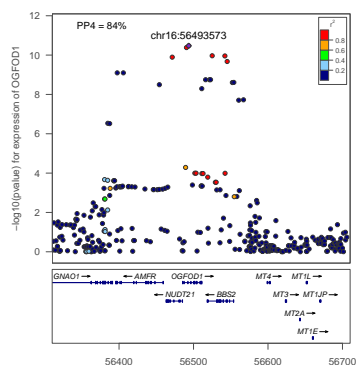
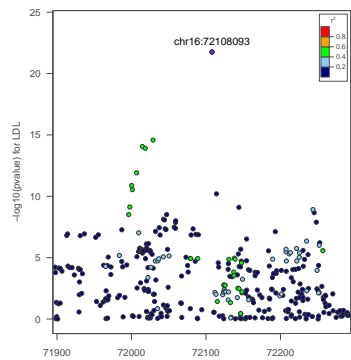
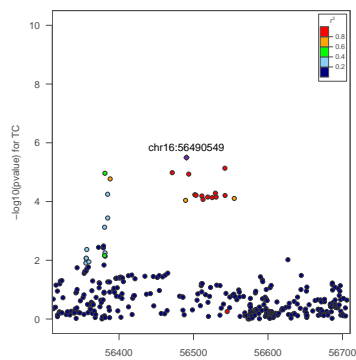
(11) CUX2/HDL

(12) CUX2/LDL



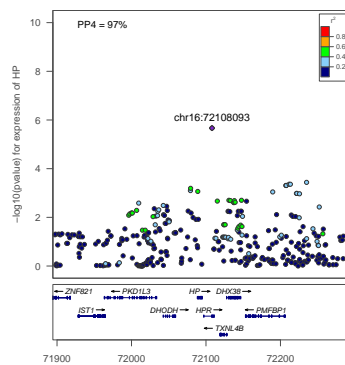
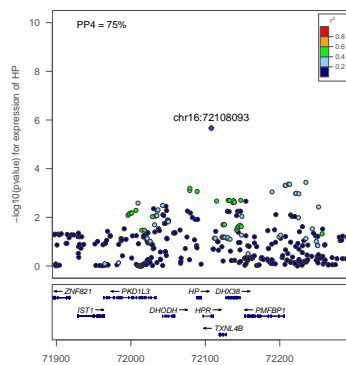
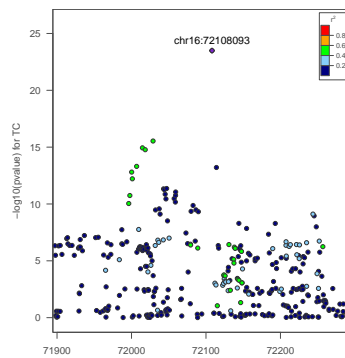
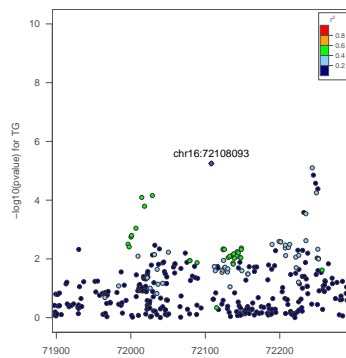
(13) CUX2/TC

(14) ENSG00000259359/HDI



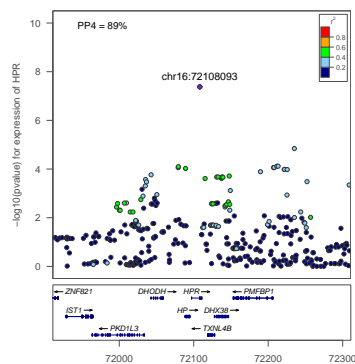
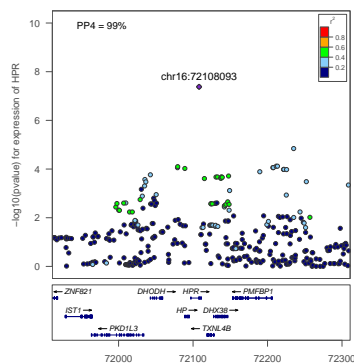
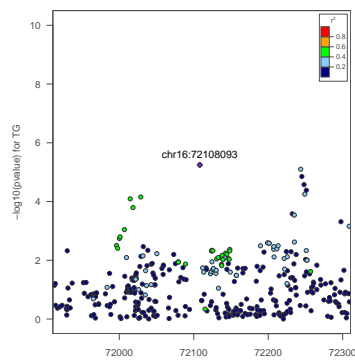
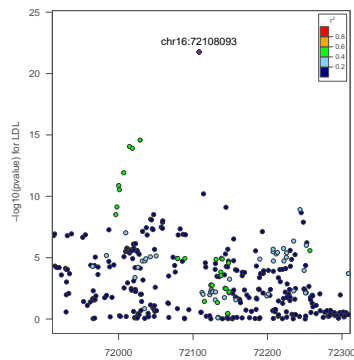
(15) OGFOD1/TC

(16) HP/LDL



(17) HP/TG

(18) HP/TC



(19) HPR/LDL

(20) HPR/TG

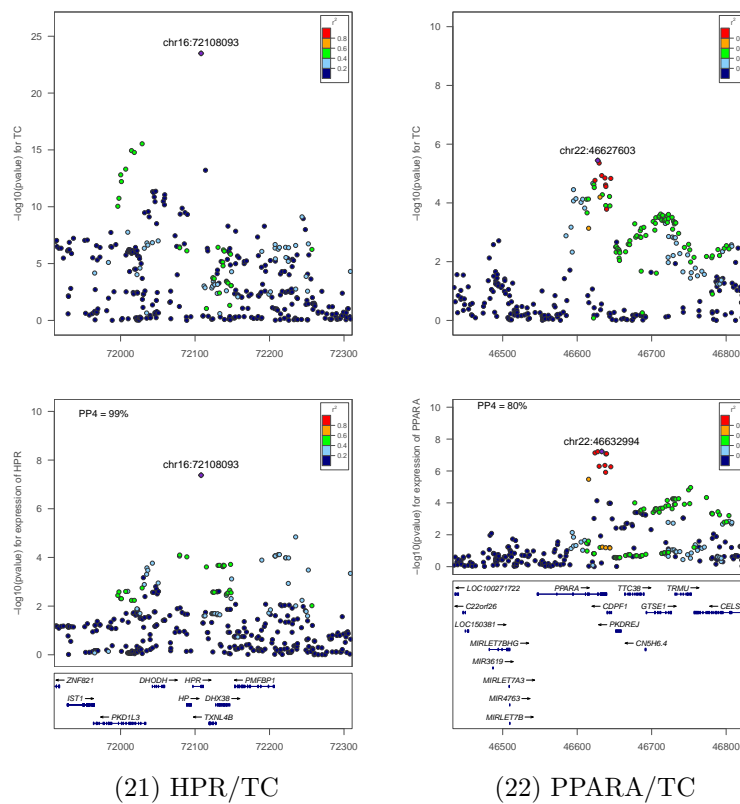


Figure S6. Regional Manhattan plots corresponding to loci listed in Table 2 of main text. Row and column headers defined as in previous figure. The genomic range may be greater than ~ 400 kilobases to improve visualisation of the signal.

Overview of gene function of new colocalisation results associated with blood lipid levels and liver expression

- *SDC1* (Syndecan-1) encodes a transmembrane heparan sulfate proteoglycan which mediates the clearance of triglyceride-rich lipoproteins in liver [16].
- *TGOLN2* (Trans-Golgi Network Protein 2) encoded by this gene regulates cholesterol transport to the trans-Golgi network and plasma membrane caveolae [17].
- *INHBB* encodes Inhibin beta B, a subunit of both activin and inhibin. This locus has been reported associated with elevated levels of lipids and cardiovascular disease risk traits [18].
- *UBXN2B* (UBX Domain Protein 2B) encodes a protein containing a UBX-domain involved in endoplasmic reticulum-associated degradation, a process which is crucial for lipid droplets maintenance [19].
- *VLDLR* (Very Low Density Lipoprotein Receptor) is known to play important roles in VLDL-triglyceride metabolism, and has been previously correlated with glucose and triglyceride plasma levels [20].
- *VIM* codes for Vimentin, and a functional role for vimentin intermediate filaments has been reported in the metabolism of lipoprotein-derived cholesterol [21].
- *CYP26A1* encodes an endoplasmic reticulum protein which regulates the the cellular level of retinoic acid, a critical signalling molecule involved in the regulation of gene expression. This protein belongs to the cytochrome P450 superfamily of enzymes which catalyse many reactions involved in maintenance of lipid homeostasis and drug metabolism [22].
- *OGFOD1* (2-oxoglutarate and iron-dependent oxygenase domain containing 1) is crucial for cellular adaptation to changes in oxygen concentration, and has been reported to function in ischaemic signalling [23].
- *HP* encodes the plasma protein haptoglobin, which binds and transports free hemoglobin (Hb) released from erythrocytes back to the liver for recycling, thereby inhibiting haemoglobin's oxidative activity [24].
- Haptoglobin-related protein (*HPR*) is a plasma protein associated with apolipoprotein-L-I containing high-density lipoprotein (HDL) particles, and has been shown to be part of the innate immune response [25].
HP and *HPR* have been previously associated with lipids [26].
- *PPARA* gene encodes the transcription factor peroxisome proliferator-activated receptor alpha (PPAR-alpha), a major regulator of lipid metabolism in the liver. PPAR-alpha serves as cellular receptor for fibrates, an anti-dyslipidemia drug that effectively lower serum triglycerides and raise serum HDL-cholesterol levels [27].

References

1. Wakefield J (2009) Bayes factors for genome-wide association studies: comparison with p-values. *Genetic Epidemiology* 33: 79–86.
2. McCullagh P, Nelder J (1983) *Generalized Linear Models*, Chapman & Hall, chapter 4.

3. Burton PR, Clayton DG, Cardon LR, Craddock N, Deloukas P, et al. (2007) Genome-wide association study of 14,000 cases of seven common diseases and 3,000 shared controls. *Nature* 447: 661–678.
4. Marchini J, Howie B, Myers S, McVean G, Donnelly P (2007) A new multipoint method for genome-wide association studies by imputation of genotypes. *Nature genetics* 39: 906–913.
5. Marchini J, Howie B (2010) Genotype imputation for genome-wide association studies. *Nature Reviews Genetics* 11: 499–511.
6. Voight BF, Kang HM, Ding J, Palmer CD, Sidore C, et al. (2012) The metabochip, a custom genotyping array for genetic studies of metabolic, cardiovascular, and anthropometric traits. *PLoS genetics* 8: e1002793.
7. Talmud PJ, Drenos F, Shah S, Shah T, Palmieri J, et al. (2009) Gene-centric association signals for lipids and apolipoproteins identified via the humanCVD beadchip. *American journal of human genetics* 85: 628.
8. Falconer DS, Mackay TFC (1996) *Introduction to Quantitative Genetics*. Longman Pub Group.
9. Vukcevic D, Hechter E, Spencer C, Donnelly P (2011) Disease model distortion in association studies. *Genetic epidemiology* 35: 278–290.
10. Guan Y, Stephens M (2008) Practical issues in imputation-based association mapping. *PLoS Genet* 4: e1000279.
11. Team RDC (2013) *R: A Language and Environment for Statistical Computing*. R Foundation for Statistical Computing, Vienna, Austria. URL <http://www.R-project.org>.
12. Autosomes Chromosome X (2012) An integrated map of genetic variation from 1,092 human genomes. *Nature* 491: 1.
13. Burren OS, Adlem EC, Achuthan P, Christensen M, Coulson RM, et al. (2011) T1dbase: update 2011, organization and presentation of large-scale data sets for type 1 diabetes research. *Nucleic acids research* 39: D997–D1001.
14. Nejentsev S, Howson JM, Walker NM, Szeszko J, Field SF, et al. (2007) Localization of type 1 diabetes susceptibility to the mhc class i genes hla-b and hla-a. *Nature* 450: 887–892.
15. Teslovich TM, Musunuru K, Smith AV, Edmondson AC, Stylianou IM, et al. (2010) Biological, clinical and population relevance of 95 loci for blood lipids. *Nature* 466: 707–713.
16. Yilmaz Y, Eren F, Colak Y, Senates E, Celikel CA, et al. (2012) Hepatic expression and serum levels of syndecan 1 (cd138) in patients with nonalcoholic fatty liver disease. *Scandinavian journal of gastroenterology* 47: 1488–1493.
17. Garver WS, Krishnan K, Gallagos JR, Michikawa M, Francis GA, et al. (2002) Niemann-pick c1 protein regulates cholesterol transport to the trans-golgi network and plasma membrane caveolae. *Journal of lipid research* 43: 579–589.
18. Johnson MP, Brennecke SP, East CE, Göring HH, Kent Jr JW, et al. (2012) Genome-wide association scan identifies a risk locus for preeclampsia on 2q14, near the inhibin, beta b gene. *PloS one* 7: e33666.
19. Wang CW, Lee SC (2012) The ubiquitin-like (ubx)-domain-containing protein ubx2/ubxd8 regulates lipid droplet homeostasis. *Journal of Cell Science* 125: 2930–2939.

20. Nasarre L, Juan-Babot O, Gastelurrutia P, Lluica-Valdeperas A, Badimon L, et al. (2012) Low density lipoprotein receptor-related protein 1 is upregulated in epicardial fat from type 2 diabetes mellitus patients and correlates with glucose and triglyceride plasma levels. *Acta diabetologica* : 1–8.
21. Sarria A, Panini S, Evans R (1992) A functional role for vimentin intermediate filaments in the metabolism of lipoprotein-derived cholesterol in human sw-13 cells. *Journal of Biological Chemistry* 267: 19455–19463.
22. Hafner M, Rezen T, Rozman D (2011) Regulation of hepatic cytochromes p450 by lipids and cholesterol. *Current drug metabolism* 12: 173–185.
23. Saito K, Adachi N, Koyama H, Matsushita M (2010) Ogfod1, a member of the 2-oxoglutarate and iron dependent dioxygenase family, functions in ischemic signaling. *FEBS letters* 584: 3340–3347.
24. Wassell J, et al. (1999) Haptoglobin: function and polymorphism. *Clinical laboratory* 46: 547–552.
25. Nielsen MJ, Petersen SV, Jacobsen C, Oxvig C, Rees D, et al. (2006) Haptoglobin-related protein is a high-affinity hemoglobin-binding plasma protein. *Blood* 108: 2846–2849.
26. Guthrie PA, Rodriguez S, Gaunt TR, Lawlor DA, Smith GD, et al. (2012) Complexity of a complex trait locus: Hp, hpr, haemoglobin and cholesterol. *Gene* 499: 8–13.
27. Staels B, Maes M, Zambon A (2008) Fibrates and future ppar α agonists in the treatment of cardiovascular disease. *Nature Clinical Practice Cardiovascular Medicine* 5: 542–553.